



**HAL**  
open science

# Local enrichment of NURBS patches using a non-intrusive coupling strategy: Geometric details, local refinement, inclusion, fracture

Robin Bouclier, Jean-Charles Passieux, Michel Salaün

## ► To cite this version:

Robin Bouclier, Jean-Charles Passieux, Michel Salaün. Local enrichment of NURBS patches using a non-intrusive coupling strategy: Geometric details, local refinement, inclusion, fracture. *Computer Methods in Applied Mechanics and Engineering*, 2016, 300, pp.1-26. 10.1016/j.cma.2015.11.007 . hal-01295461

**HAL Id: hal-01295461**

**<https://hal.science/hal-01295461>**

Submitted on 31 Mar 2016

**HAL** is a multi-disciplinary open access archive for the deposit and dissemination of scientific research documents, whether they are published or not. The documents may come from teaching and research institutions in France or abroad, or from public or private research centers.

L'archive ouverte pluridisciplinaire **HAL**, est destinée au dépôt et à la diffusion de documents scientifiques de niveau recherche, publiés ou non, émanant des établissements d'enseignement et de recherche français ou étrangers, des laboratoires publics ou privés.

# Local enrichment of NURBS patches using a non-intrusive coupling strategy: geometric details, local refinement, inclusion, fracture

Robin Bouclier<sup>a</sup>, Jean-Charles Passieux<sup>b</sup>, Michel Salaün<sup>b</sup>

<sup>a</sup> *Université de Toulouse, Institut de Mathématiques de Toulouse, UMR CNRS 5215, INSA-Toulouse, 135 avenue de Rangueil, F-31077 Toulouse Cedex 04, France*

<sup>b</sup> *Université de Toulouse, Institut Clément Ader, FRE CNRS 3687 INSA/UPS/ISAE/Mines Albi, 3 rue Caroline Aigle, 31400 Toulouse, France*

---

## Abstract

In this work, we apply a non-intrusive global/local coupling strategy for the modelling of local phenomena in a NURBS patch. The idea is to consider the NURBS patch to be enriched as the global model. This results in a simple, flexible strategy: first, the global NURBS patch remains unchanged, which completely eliminates the need for costly re-parametrization procedures (even if the local domain is expected to evolve); then, easy merging of a linear NURBS code with any other existing robust codes suitable for the modelling of complex local behaviour is possible. The price to pay is the number of iterations of the non-intrusive solver but we show that this can be strongly reduced by means of acceleration techniques. The main development for NURBS is to be able to handle non-conforming geometries. Only slight changes in the implementation process, including the setting up of suitable quadrature rules for the evaluation of the interface reaction forces, are made in response to this issue. A range of numerical examples in two-dimensional linear elasticity are given to demonstrate the performance of the proposed methodology and its significant potential to treat any case of local enrichment in a NURBS patch simply.

*Keywords:* Isogeometric analysis, NURBS, Non-intrusive coupling, Domain

---

*Email addresses:* `robin.bouclier@math.univ-toulouse.fr` (Robin Bouclier), `passieux@insa-toulouse.fr` (Jean-Charles Passieux), `michel.salaun@isae.fr` (Michel Salaün)

## 1. Introduction

With the introduction of IsoGeometric Analysis (IGA) (see Hughes *et al.* [1] for the first contribution and Cottrell *et al.* [2] for a detailed account), it has become possible to compute structures using the exact geometry of the Computer-Aided Design (CAD) model regardless of the mesh density. For this purpose, Lagrange polynomials are replaced by Non-Uniform-Rational-B-Spline (NURBS) functions to perform the analysis. NURBS functions have a higher order of continuity, namely  $C^{(p-1)}$  through the knot-span elements of the mesh for a polynomial degree  $p$ , which, on a per-degree-of-freedom basis, gives increased accuracy in comparison with standard Finite Element Methods (FEM) (see, *e.g.*, [3] for a theoretical analysis, [4] for applications in structural vibrations, [5] for problems of standard elasticity, [6] for embedded domain methods and [7, 8] for shell analysis). Although the global accuracy of NURBS is now proved, the rigid tensor product structure of these functions still prevents simple modelling of local behaviours in a NURBS patch. For example, the integration of geometric details (*i.e.*, basically, holes) leads to the analysis of a trimmed NURBS patch, which is not a trivial task. The basic strategy may involve a re-parametrization of the NURBS model, including the splitting of the new geometry into several patches with  $C^0$  continuity at the boundaries. This may apply not only for geometric details but to all situations of local models different from the global NURBS patch model (*e.g.*, local refinement, inclusion [9], local fracture [10, 11], local plasticity [12], etc.). This entails a considerable modelling effort that is often as complex and time consuming as standard mesh generation and so is opposed to the core idea of IGA, which advocates a direct link between geometry and analysis.

After the pioneering works on NURBS-based IGA, great interest in methods addressing these modelling questions has emerged in the field. One of the most noteworthy is the development of new splines that enable local refinement: hierarchical B-splines and NURBS [13, 14], LRB-splines [15], T-splines [16, 17] and multigrid-based NURBS [18]. Among these strategies, T-splines seem to have gathered considerable momentum in both the computational geometry and analysis communities since they also appear suitable to address trimmed multi-patch geometries. Nevertheless, the implementation of these new IGA techniques can appear complex and additional efforts

may be necessary to solve the issue of describing a local behaviour that is different from the global behaviour (inclusion, local fracture, local plasticity).

Concurrently, a second recent approach initiated in Nguyen *et al.* [9] and Ruess *et al.* [19] and based on the combination of the Finite Cell Method (FCM) with Nitsche coupling may constitute an interesting option to resolve our problem of modelling local behaviours in a NURBS patch. The FCM, which combines the fictitious domain approach with higher-order finite elements and adaptive integration, has proved to be efficient for the analysis of any arbitrary trimmed patches (see, *e.g.*, [20] for a detailed review). Regarding NURBS coupling, a great effort has been made concerning the connection of NURBS patches in recent years. One of the first works on the subject was certainly that of Hesch and Betsch [21], who used the Lagrange multiplier method to couple NURBS solids. Then, a comparative study in Apostolatos *et al.* [22] showed the efficiency of a Nitsche-based technique for NURBS. In consequence, Nitsche coupling has been used for connecting 3D NURBS patches [9], for 3D-plate NURBS coupling [23, 24], and with NURBS immersed boundary methods [25, 19]. Although it appears interesting because of the strong mathematics behind it and the absence of additional degrees of freedom, the Nitsche method leads to considerable implementation work and an increased cost of computation, since an additional eigenvalue problem has to be solved for the stabilizing term. As a result, Dornisch *et al.* [26] has recently developed a weak substitution method that can be interpreted as a mortar method. Although the combination of the FCM with Nitsche coupling may be promising, the drawback of such a strategy, if directly applied to the local enrichment of a NURBS patch, is that it suffers from some intrusiveness. More precisely, two main limitations can be highlighted. On the one hand, the introduction of a local zone within the NURBS patch requires a re-parametrization of the global geometric model, which is not a trivial task in the NURBS framework. This can be very time consuming, in particular when the local region is expected to evolve (*e.g.*, shape optimization of the geometric details, of the inclusions, crack propagation, expansion of the plastic zone) since several re-constructions and re-computations of the whole problem then have to be performed during the simulation. On the other hand, it is to be noted that, when Nitsche-based methods are used, both the global and local operators have to be modified and merged together for the coupling, which implies significant implementation efforts and a monolithic resolution and thus prevents the simple use of existing robust codes for the global/local strategy.

To overcome this difficulty, the alternative purpose of this work is to make use of a non-intrusive global/local coupling strategy that has become popular in FEM. Based on the idea of Whitcomb [27], formalized later by Gendre *et al.* [12], for the modelling of local plasticity, the method that we consider in this work involves the definition of two finite element models: a global, coarse model of the whole structure and a local, more detailed "sub-model" meant to replace the global model in the area of interest. An iterative coupling technique is used to perform the substitution in an exact but non-intrusive way: only interface data are transmitted from one model to the other and the global stiffness operator remains unchanged (independently of the shape of the local domain). This strategy has been applied in FEM for the modelling of crack propagation [11], for the modelling of localized uncertainties [28], for 3D-plate coupling [29] and for nonlinear domain decomposition [30]. Let us note that this methodology, involving the coupling of a global model and a local model in an iterative manner, has similarities with some hierarchical global/local methods in FEM: for example, the Chimera method [31], the method of finite element patches [32], numerical zoom [33] or the  $hp - d$  method [34, 35, 36]. However, the difference of the strategy considered here is that the contribution of the global solution in the local area is totally replaced by the local solution while, in the hierarchical strategy, an approximate solution is sought as the sum of the global coarse contribution and a local fine one. As a result, the advantage of the algorithm used is that it reduces the interactions between global and local discretizations. In the proposed approach, the two models talk to each other with interface integrals only, while the evaluation of mixed terms over the whole local domain is necessary in the hierarchical approach. In this sense, the strategy followed in this work is said to be non-intrusive.

In this paper, we propose an application of the non-intrusive technique [27, 12, 11, 28, 29, 30] to the NURBS context. The idea is to take the NURBS patch to be enriched as the global model. In consequence, the global patch is never modified during the simulation, which eliminates the need for costly NURBS re-parametrization procedures. In addition, the global stiffness operator is assembled and factorized only once and the system to be solved remains well-conditioned. If the local behaviour is expected to evolve, only the local model (including a limited number of degrees of freedom since restricted to a thin zone of the structure) has to be re-computed. Moreover, it should be mentioned that the flexibility of the strategy allows simple modelling of a variety of local behaviours. Since the global and local problems are

solved alternately in a non-intrusive strategy, two different numerical codes can be used to compute the global and local models. Thus, a linear NURBS code can be used for the global modelling of the NURBS patch while any other existing robust code integrating any other numerical method can be used to incorporate an accurate local model. By making use of this strategy, we are able to address geometric details (for which the local model is void: it represents holes) as well as all other cases of local models that are covered: *e.g.*, refined mesh, inclusion, fracture, plasticity. In particular, we successfully apply the non-intrusive approach in this work for the situation of holes, local refinement, inclusion and local fracture in a two-dimensional NURBS patch under linear elasticity.

The difficulty when applying the non-intrusive strategy to NURBS is that non-conforming geometries need to be addressed. By non-conforming geometries, we mean that the local model domain overlaps the knot-span elements in the global NURBS patch as the local model domain may be bounded by a trimming curve living in the interior of the global NURBS patch to be enriched. Thus, given the rigid tensor product structure of the NURBS, there is no reason for the boundary of the local model domain to be aligned with the edges of the global NURBS patch elements. The non-conforming geometries issue does not involve specific modifications of the equations and associated weak forms but special attention is needed in the implementation process. In particular, the evaluation of the reaction forces of the complement part of the global model (the part meant to be replaced in the non-intrusive algorithm) requires the setting up of a suitable quadrature rule and its treatment in the global NURBS patch. For this purpose, an exact NURBS domain is simply constructed from the NURBS trimming curve in the case of a geometric detail while the quadrature rule used for the local model is transposed within the global NURBS patch in the case of real (covered) local models. With regard to coupling, an application of the conventional Lagrange multiplier approach to non-conforming geometries is employed to meet the non-intrusive constraint in the sense of [11, 29, 30]. Acceleration techniques, such as techniques based on Aitken’s Delta Squared method or a Quasi-Newton method (see, *e.g.*, [30]), are also implemented in the present situation, which results in a significant reduction of the number of iterations of the non-intrusive algorithm.

The paper is organized as follows: after this introduction, Section 2 reviews the fundamentals of NURBS-based IGA and introduces the reference global/local coupling problem to be solved. Then, Section 3 is devoted to the

application of the non-intrusive global/local strategy to the NURBS context. In particular, the study is divided into two parts: the situation of geometric details involving a void local model is investigated before the more usual case of covered local models is addressed. Section 4 presents a range of numerical examples in two-dimensional linear elasticity that demonstrate the performance of our methodology and its significant potential for the simple treatment of any case of local enrichment in a NURBS patch. Finally, Section 5 concludes on this work by summarizing our most important points and motivating future research in this direction.

## 2. The reference problem

This section establishes the context of the study and introduces the corresponding notations. We start with a brief review of the concept of NURBS-based IGA with a particular emphasis on the trimming concept that may facilitate the geometric modelling of local behaviours. Then, the reference global/local problem is presented along with its standard weak coupling formulation.

### 2.1. NURBS-based isogeometric analysis

#### 2.1.1. Basics.

For the discretization, we will use the recent concept of IGA based on NURBS functions. Only the fundamentals of the concept are given in the following. For further details, the interested reader is referred to the references cited below.

The NURBS concept was first introduced in Hughes *et al.* [1] and formalized more recently in the book by Cottrell *et al.* [2]. NURBS functions are a generalized version of B-spline functions and have become a standard for geometric modelling in CAD and computer graphics (see, for example, Cohen *et al.* [37], Piegl and Tiller [38], Farin [39] and Rogers [40]). These functions lend themselves to an exact representation of many shapes used in engineering, such as conical sections. They can be viewed as rational projections of higher-order B-splines and, therefore, they possess many of the properties of B-splines, the most interesting one being their high degree of continuity.

For the presentation in this part, we consider a domain in 3D so as to be general. If  $(N_A)_{A \in \{1, 2, \dots, n\}}$  denote the  $n$  3D NURBS functions,  $(\omega_A)_{A \in \{1, 2, \dots, n\}}$  the associated weights and  $(P_A)_{A \in \{1, 2, \dots, n\}}$  the associated control points of

coordinates  $(\mathbf{x}_A)_{A \in \{1, 2, \dots, n\}}$  in the global coordinate system, the geometry of the structure is described through the position vector  $\mathbf{M}$  defined as:

$$\mathbf{M} = \sum_{A=1}^n N_A \mathbf{x}_A, \quad (1)$$

where the NURBS functions are obtained from the B-spline functions  $(\bar{N}_A)_{A \in \{1, 2, \dots, n\}}$  such that:

$$N_A = \frac{\bar{N}_A w_A}{\sum_{A=1}^n \bar{N}_A w_A}. \quad (2)$$

Now, all one needs to do in order to define the 3D B-spline functions  $\bar{N}_A$  at control point  $P_A$  is to perform the tensor product of the 1D B-spline functions associated with this point in the three spatial directions. If one denotes  $(M_i^1)_{i \in \{1, 2, \dots, n_1\}}$ ,  $(M_j^2)_{j \in \{1, 2, \dots, n_2\}}$  and  $(M_k^3)_{k \in \{1, 2, \dots, n_3\}}$  the  $n_1$ ,  $n_2$  and  $n_3$  1D B-spline functions associated with each of the three spatial directions, this means that at control point  $P_A$ , which corresponds to the  $i^{\text{th}}$ ,  $j^{\text{th}}$  and  $k^{\text{th}}$  control points in these directions, one has:

$$\bar{N}_A = M_i^1 \times M_j^2 \times M_k^3. \quad (3)$$

The 1D B-spline functions are defined using a knot vector. Each knot vector associated with a direction is defined in the parametric domain. For example, for the first direction, one takes knot vector  $\Xi = \{\xi_1, \xi_2, \dots, \xi_{n_1+p+1}\}$ , where  $\xi_l \in \mathbb{R}$  is the  $l^{\text{th}}$  knot, with  $l$  being the knot index ( $l = 1, 2, \dots, n_1 + p + 1$ ) and  $p$  the polynomial degree of the functions  $(M_i^1)_{i \in \{1, 2, \dots, n_1\}}$ . The knots divide the parametric space into elements, and the interval  $\{\xi_1, \xi_{n_1+p+1}\}$  constitutes the IGA patch. The patch may be thought of as a macro-element. Most geometries utilized for academic test cases can be modeled with a single patch. In two-dimensional topologies, a patch is a rectangle in the parametric domain. In three dimensions it is a cuboid.

**Remark 1.** *In this work, we need to be careful with the term "patch" since this one can be employed for both NURBS and global/local coupling algorithm. We emphasize here that the term "patch" will only refer to the concept of IGA patch in the following. Thus, the term patch will never refer to the local model (in opposition to [32] for example).*

Unlike standard FEM where each element has its own parametrization,

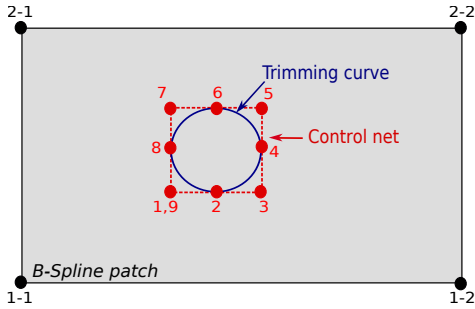
the parametric space of B-Spline functions is localized onto the patch. There can be more than one knot at a given location of the parametric space. If  $m$  is the multiplicity of the considered knot, the functions have  $C^{p-m}$  continuity at that location. If the knots are evenly spaced, the knot vector is said to be uniform. A knot vector whose first and last knots have multiplicity  $p + 1$  is said to be open. In this case, the basis is interpolating at the boundary knots of the interval, which facilitates the application of the boundary conditions. For the sake of simplicity, we will consider in this work geometries that can be represented (excluding the local details) with the use of only one patch. Furthermore only open uniform knot vectors will be considered. The 1D B-spline basis functions for a given order  $p$  are defined recursively from the knot vector using the Cox-de Boor recursion formula (see, for example, Cohen *et al.* [37]).

To take advantage of the superior approximation properties of NURBS functions, one chooses them to be at least of polynomial degree two in all the spatial directions. As far as continuity is concerned, one performs  $k$ -refinement, meaning that one adds elements while keeping the higher degree of continuity of the NURBS functions, namely  $C^{p-1}$  at the knot level. The positions of the control points and the values of the associated weights can be adjusted in order to build conical sections exactly, after which these geometries are preserved through mesh refinement. For a good overview of mesh generation and refinement, see Cottrell *et al.* [41].

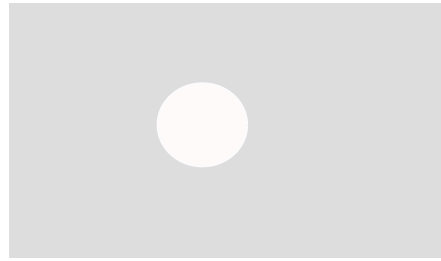
### 2.1.2. The trimming concept.

The difficulty to model local behaviours in a NURBS patch is due to the use of the tensor product (see Eq. 3). For example, this makes the integration of geometric details (*e.g.*, holes) in a NURBS patch far from trivial. Indeed, since standard IGA technology requires a boundary fitted discretization for the analysis, a re-parametrization of the whole NURBS model taking into account the geometric detail is required. This may lead to the splitting of the new geometry into several patches with  $C^0$  continuity at the boundaries. This entails a considerable modelling effort, which is often as complex and time consuming as standard mesh generation as explained in [19]. In CAD programs, where the only need is the rendering of the geometry, such a re-parametrization is not necessary. Designers make use of the trimming concept to create an almost unlimited range of geometric shapes. The trimming concept is illustrated in 2D for the situation of a circular hole as the geometric detail of a rectangular structure, see Fig. 1.

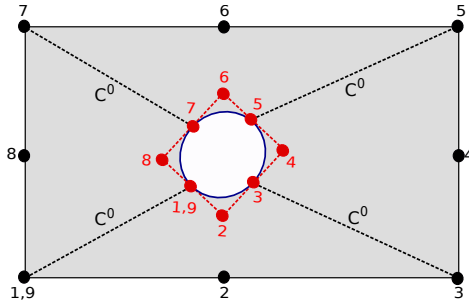
This surface can be classified as a trimmed surface. Its description is simply given by: a one-patch B-Spline surface parametrization for the plate (without the hole) and a NURBS curve parametrization for the trimming curve that forms the boundary of the hole. The trimming curve specifies visible and invisible regions on the surface patch. As a consequence, the underlying NURBS patch remains unaffected by the trimming object and preserves its topology. Conversely, the NURBS parametrization of the plate including the hole (without trimming) is shown in Fig. 1(c). As can be seen, a NURBS re-parametrization of the geometry (including the splitting into 4 elements with  $C^0$  continuity on the boundary) is necessary.



(a) NURBS parametrization of the trimmed geometry.



(b) CAD rendering.



(c) NURBS re-parametrization (without trimming).

Figure 1: Illustration of the trimming concept.

## 2.2. Definition of the global/local problem

### 2.2.1. Governing equations.

We undertake to study a multi-domain model characterized by a physical domain  $\Omega \in \mathbb{R}^d$ ,  $d = 2$  or  $3$ , which is divided into two disjoint, open and

bounded subsets  $\Omega_{11}$  and  $\Omega_2$  such that  $\Omega = \Omega_{11} \cup \Omega_2$  and  $\Omega_{11} \cap \Omega_2 = \emptyset$ . Those two non-overlapping subdomains share a common interface denoted  $\Gamma$  (see Fig. 2).

**Remark 2.** *As subdomains are open, one would need to write  $\bar{\Omega} = \bar{\Omega}_{11} \cup \bar{\Omega}_2$  to be rigorous. In the paper, we decide to omit this notation in order to ease the reading.*

We suppose that the local part of the problem is the small region  $\Omega_2$  and that a simple linear elastic model is sufficient to describe the global behaviour in the complement domain  $\Omega_{11}$ . Even if the method applies in more general context, we assume in this work a linear elastic constitutive law in  $\Omega_2$  as well. We emphasize that  $\Omega_2$  may also constitute a geometric detail (*i.e.*, basically, a hole). To obtain this situation, one simply needs to take the Hooke tensor in region  $\Omega_2$  equal to zero. Regarding the NURBS discretization of the problem, domain  $\Omega$  may constitute a NURBS patch and  $\Gamma$  (and so the extension to  $\partial\Omega_2$ ) may be viewed as a trimming curve that enables to specify the local part  $\Omega_2$ . Domains  $\Omega_{11}$  and  $\Omega_2$  are subjected to body forces  $\mathbf{f}_{11}^g$  and  $\mathbf{f}_2^g$ , respectively. Furthermore, surface forces  $\mathbf{F}_{11}^g$  and  $\mathbf{F}_2^g$  are associated to boundaries  $\Gamma_{F_{11}}$  and  $\Gamma_{F_2}$  and, displacements  $\mathbf{u}_{11}^g$  and  $\mathbf{u}_2^g$  are prescribed over boundaries  $\Gamma_{u_{11}}$  and  $\Gamma_{u_2}$ . The boundaries satisfy the following relations :

$$\left\{ \begin{array}{l} \Gamma_{F_m} \cup \Gamma_{u_m} \cup \Gamma = \partial\Omega_m \\ \Gamma_{F_m} \cap \Gamma_{u_m} = \emptyset \\ \Gamma_{F_m} \cap \Gamma = \emptyset \\ \Gamma_{u_m} \cap \Gamma = \emptyset \end{array} \right. \quad \text{with } m = 11 \text{ and } 2.$$

**Remark 3.** *We emphasize that we restrict ourselves to a domain  $\Omega$  that can be represented using a single NURBS patch for simplicity in the presentation only. Obviously, the strategy developed in this work straightforwardly applies for the more general case of a multi-patch geometric model.*

The problem to be solved is a classical multi-domain linear elastic problem in  $\Omega_{11} \cup \Omega_2$ . In each subdomain, the kinematic constraints, the equilibrium equations and the constitutive relations have to be verified. Using the subscript  $m$  to denote a quantity that is valid over region  $\Omega_m$ , with  $m = 11$  and

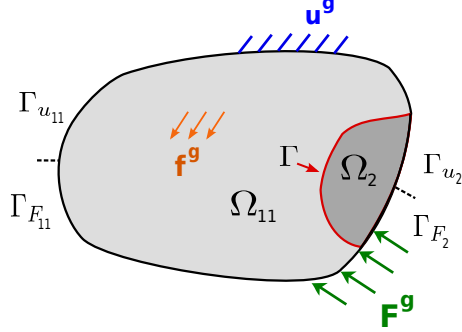


Figure 2: The reference global/local problem.

2, the corresponding governing equations read:

$$\begin{cases} \mathbf{u}_m = \mathbf{u}_m^g & \text{over } \Gamma_{u_m} ; \\ \mathbf{div}(\underline{\underline{\sigma}}_m) + \mathbf{f}_m^g = \mathbf{0} & \text{in } \Omega_m ; \\ \underline{\underline{\sigma}}_m \mathbf{n}_m = \mathbf{F}_m^g & \text{over } \Gamma_{F_m} ; \\ \underline{\underline{\sigma}}_m = \underline{\underline{\underline{C}}}_m \underline{\underline{\underline{\varepsilon}}}(\mathbf{u}_m) & \text{in } \Omega_m. \end{cases} \quad (4)$$

For the sake of readability, we decided to use bold symbols for first-order tensors while we underline twice the second- and four times the fourth-order tensors. In the above equations,  $\underline{\underline{\underline{\varepsilon}}}(\mathbf{u}_m)$  denotes the infinitesimal strain tensors,  $\underline{\underline{\sigma}}_m$  the Cauchy stress tensors and  $\underline{\underline{\underline{C}}}_m$  the Hooke tensors.  $\mathbf{n}_{11}$  and  $\mathbf{n}_2$  represent the outward unit normals to  $\Omega_{11}$  and  $\Omega_2$ , respectively. To complete the formulation of the boundary value problem, the following coupling conditions have to be added:

$$\begin{cases} \mathbf{u}_{11} - \mathbf{u}_2 = \mathbf{0} & \text{on } \Gamma ; \\ \underline{\underline{\sigma}}_{11} \mathbf{n}_{11} + \underline{\underline{\sigma}}_2 \mathbf{n}_2 = \mathbf{0} & \text{on } \Gamma. \end{cases} \quad (5)$$

They ensure kinematic compatibility between the coupled domains and equilibrium of the tractions along the coupling interface  $\Gamma$ , respectively.

### 2.2.2. Weak form.

The starting point in the derivation of a non-intrusive strategy in the sense of [11, 29, 30] is to weakly formulate the coupling problem (4)-(5) with a Lagrange multiplier approach. The development of the non-intrusive

coupling formulation is not the subject of this section. Nevertheless, since it is based on the use of a Lagrange multiplier approach, the corresponding classical weak coupling formulation is given here. A standard fixed point solver is also presented to account for the possibility to dissociate  $\Omega_{11}$  and  $\Omega_2$  in the resolution. These developments constitute the reference formulation and the standard global/local solver of our coupling problem.

We start by defining the functional spaces  $\mathcal{U}_m$  and  $\mathcal{V}_m$  over domain  $\Omega_m$  that will contain the solution and trial functions respectively:

$$\mathcal{U}_m = \left\{ \mathbf{u}_m \in [H^1(\Omega_m)]^d, \mathbf{u}_m|_{\Gamma_{u_m}} = \mathbf{u}_m^{\mathbf{g}} \right\}; \mathcal{V}_m = \left\{ \mathbf{v}_m \in [H^1(\Omega_m)]^d, \mathbf{v}_m|_{\Gamma_{u_m}} = \mathbf{0} \right\}. \quad (6)$$

We also introduce  $\mathcal{M} \subset [L^2(\Gamma)]^d$  the space for the Lagrange multiplier. The formulation involves the set up of the following Lagrangian:

$$L((\mathbf{u}_{11}, \mathbf{u}_2), \boldsymbol{\lambda}) = \frac{1}{2}a_{11}(\mathbf{u}_{11}, \mathbf{u}_{11}) + \frac{1}{2}a_2(\mathbf{u}_2, \mathbf{u}_2) - l_{11}(\mathbf{u}_{11}) - l_2(\mathbf{u}_2) + b(\boldsymbol{\lambda}, \mathbf{u}_{11} - \mathbf{u}_2), \quad (7)$$

where bilinear form  $a_m$  and linear form  $l_m$  associated to domain  $\Omega_m$  read:

$$\begin{cases} a_m(\mathbf{u}_m, \mathbf{v}_m) = \int_{\Omega_m} \underline{\underline{\varepsilon}}(\mathbf{v}_m) : \underline{\underline{C}}_m \underline{\underline{\varepsilon}}(\mathbf{u}_m) \, d\Omega_m; \\ l_m(\mathbf{v}_m) = \int_{\Omega_m} \mathbf{v}_m \cdot \mathbf{f}_m^{\mathbf{g}} \, d\Omega_m + \int_{\Gamma_{F_m}} \mathbf{v}_m \cdot \mathbf{F}_m^{\mathbf{g}} \, d\Gamma_{F_m}; \end{cases} \quad (8)$$

and with bilinear form  $b$  defined such that:

$$b(\boldsymbol{\mu}, \mathbf{u}) = \int_{\Gamma} \boldsymbol{\mu} \cdot \mathbf{u} \, d\Gamma. \quad (9)$$

With above notations, the resulting variational formulation of the coupled problem can be written as follows:

Find  $\mathbf{u}_{11} \in \mathcal{U}_{11}$ ,  $\mathbf{u}_2 \in \mathcal{U}_2$ , and  $\boldsymbol{\lambda} \in \mathcal{M}$  such that:

$$\begin{cases} a_{11}(\mathbf{u}_{11}, \mathbf{v}_{11}) + b(\boldsymbol{\lambda}, \mathbf{v}_{11}) = l_{11}(\mathbf{v}_{11}), & \forall \mathbf{v}_{11} \in \mathcal{V}_{11}; \\ a_2(\mathbf{u}_2, \mathbf{v}_2) - b(\boldsymbol{\lambda}, \mathbf{v}_2) = l_2(\mathbf{v}_2), & \forall \mathbf{v}_2 \in \mathcal{V}_2; \\ b(\boldsymbol{\mu}, \mathbf{u}_{11} - \mathbf{u}_2) = 0, & \forall \boldsymbol{\mu} \in \mathcal{M}. \end{cases} \quad (10)$$

Rather than directly solving equation (10) (*i.e.*, in a monolithic way), an

asymmetric algorithm, where Neumann problems over  $\Omega_{11}$  and Dirichlet problems over  $\Omega_2$  are alternatively solved until convergence, may also be used. This leads to the standard global/local algorithm. For the  $n^{\text{th}}$  iteration, we can proceed as follows: starting with  $\boldsymbol{\lambda}^{(0)} \in \mathcal{M}$ , we look for  $\mathbf{u}_{11}^{(n)} \in \mathcal{U}_{11}$ ,  $\mathbf{u}_2^{(n)} \in \mathcal{U}_2$ , and  $\boldsymbol{\lambda}^{(n)} \in \mathcal{M}$  such that:

1. Resolution of a Neumann problem over  $\Omega_{11}$ :

$$a_{11}(\mathbf{u}_{11}^{(n)}, \mathbf{v}_{11}) = l_{11}(\mathbf{v}_{11}) - b(\boldsymbol{\lambda}^{(n-1)}, \mathbf{v}_{11}), \quad \forall \mathbf{v}_{11} \in \mathcal{V}_{11}. \quad (11)$$

2. Resolution of a Dirichlet problem over  $\Omega_2$ :

$$\begin{cases} a_2(\mathbf{u}_2^{(n)}, \mathbf{v}_2) - b(\boldsymbol{\lambda}^{(n)}, \mathbf{v}_2) = l_2(\mathbf{v}_2), & \forall \mathbf{v}_2 \in \mathcal{V}_2; \\ b(\boldsymbol{\mu}, \mathbf{u}_2^{(n)}) = b(\boldsymbol{\mu}, \mathbf{u}_{11}^{(n)}), & \forall \boldsymbol{\mu} \in \mathcal{M}. \end{cases} \quad (12)$$

The global/local algorithm (11)-(12) has the drawback to be intrusive. Indeed, it is important to note that the stiffness operator  $a_{11}$  depends at this stage on the interface  $\Gamma$  or, in other words, on the shape of the local domain  $\Omega_2$ . As a consequence, if domain  $\Omega_2$  has to evolve (during optimization process, or crack propagation for instance), not only the local operator  $a_2$  but also the global operator  $a_{11}$  have to be fully re-built and factorized. This can be very time consuming and especially in the NURBS framework since the strategy would involve several re-parametrizations of the global NURBS patch. To overcome the difficulty, the purpose of this work is to make use of the non-intrusive coupling [27]. This is the object of the next section.

### 3. The global/local non-intrusive strategy

#### 3.1. Principle

Rather than considering only a part of the NURBS patch (region  $\Omega_{11}$ ) as the domain containing the global model, the idea of non-intrusive coupling is to involve a global model defined over the whole existing NURBS patch. The situation is illustrated in Fig. 3. In order to do this, domain  $\Omega_{12}$  is introduced to characterize the region in which the global model of  $\Omega_{11}$  is fictively prolonged.  $\Omega_{12}$  is defined in such a way that the NURBS patch domain is covered by  $\Omega_{11} \cup \Omega_{12}$ . From here on, we refer to domain  $\Omega_1 = \Omega_{11} \cup \Omega_{12}$  to characterize the global NURBS patch that contains the global model everywhere. We proceed in the same way with the boundaries by introducing  $\Gamma_{u_1} = \Gamma_{u_{11}} \cup \Gamma_{u_{12}}$  for the prescribed displacements and  $\Gamma_{F_1} = \Gamma_{F_{11}} \cup \Gamma_{F_{12}}$  for

the applied forces. The objective of the non-intrusive strategy is then to replace the global model over  $\Omega_{12}$  by the local one in  $\Omega_2$  without actually modifying the global NURBS patch operators over  $\Omega_1$ .

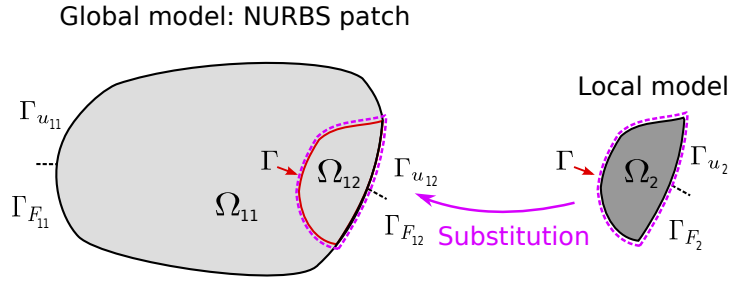


Figure 3: The non-intrusive global/local problem.

For the construction of the non-intrusive strategy, we proceed in two parts. Each of the parts has its own application. In the first part, we consider the particular case of the non-intrusive modelling of geometric details in a NURBS patch. Domain  $\Omega_2$  is then assumed to be a hole that is bounded by a trimming curve. In this case, the local model is said to be "void". In the second part, we investigate the more usual situation of a covered local model that behaves differently from the global model. In contrast to "void" models, we refer to "covered" local models in the second case. Fig. 4 shows the problems to be solved for the two cases.

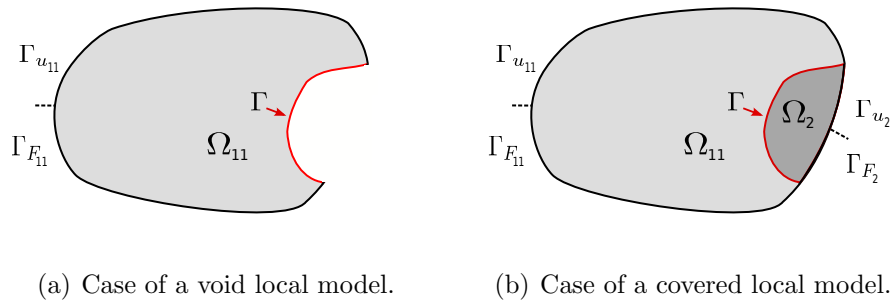


Figure 4: Problems to be solved using the non-intrusive strategy.

### 3.2. Part 1: Case of "void" local models

#### 3.2.1. The continuum version.

In the case of a void local model (see Fig. 4(a)), the equations related to domain  $\Omega_2$  vanish in the reference problem (4)-(5). Taking into account these simplifications in Eq. (10) leads to the following usual weak form for the new problem:

$$\begin{cases} \text{Find } \mathbf{u}_{11} \in \mathcal{U}_{11} \text{ such that:} \\ a_{11}(\mathbf{u}_{11}, \mathbf{v}_{11}) = l_{11}(\mathbf{v}_{11}), \quad \forall \mathbf{v}_{11} \in \mathcal{V}_{11}. \end{cases} \quad (13)$$

To derive the corresponding non-intrusive formulation, we first perform a continuous prolongation of the displacement solution from  $\Omega_{11}$  to  $\Omega_{12}$ . There are (in principle) infinitely many possible prolongations but an arbitrary prolongation can be used for the formulation of the method. From a practical point of view, we define  $\mathbf{u}_1$  the prolongation of  $\mathbf{u}_{11}$  to the full domain  $\Omega_1$  such that:

$$\mathbf{u}_1 \in [H^1(\Omega_1)]^d \Leftrightarrow \mathbf{u}_1 = \begin{cases} \mathbf{u}_{11} \in [H^1(\Omega_{11})]^d \\ \mathbf{u}_{12} \in [H^1(\Omega_{12})]^d \end{cases} \quad \text{and} \quad \mathbf{u}_{11}|_{\Gamma} = \mathbf{u}_{12}|_{\Gamma}. \quad (14)$$

$\mathbf{u}_{12}$  corresponds to the prolonged part of the global solution  $\mathbf{u}_1$  to domain  $\Omega_{12}$ . As well, we introduce  $\mathbf{f}_{12}^g = \mathbf{f}_2^g$ ,  $\mathbf{F}_{12}^g = \mathbf{F}_2^g$  and  $\mathbf{u}_{12}^g = \mathbf{u}_2^g$  the fictitious prolongation of  $\mathbf{f}_{11}^g$ ,  $\mathbf{F}_{11}^g$  and  $\mathbf{u}_{11}^g$  to  $\Omega_{12}$ ,  $\Gamma_{F_{12}}$  and  $\Gamma_{u_{12}}$ , respectively. In this specific case of a void local model, we may take  $\mathbf{f}_{12}^g = \mathbf{0}$ ,  $\mathbf{F}_{12}^g = \mathbf{0}$  and  $\mathbf{u}_{12}^g = \mathbf{0}$ . With these notations, we can reformulate problem (13) over  $\Omega_1$  as follows:

$$\begin{cases} \text{Find } \mathbf{u}_1 \in \mathcal{U}_1 \text{ such that:} \\ a_1(\mathbf{u}_1, \mathbf{v}_1) = a_1(\mathbf{u}_1, \mathbf{v}_1) + \{l_{11}(\mathbf{v}_1) - a_{11}(\mathbf{u}_1, \mathbf{v}_1)\}, \quad \forall \mathbf{v}_1 \in \mathcal{V}_1, \end{cases} \quad (15)$$

where the functional spaces  $\mathcal{U}_1$  and  $\mathcal{V}_1$  and the bilinear form  $a_1$  are defined over  $\Omega_1$  using the formalism of Eqs. (6) and (8), respectively. Then, we can make use of the additivity of the integral with respect to domain  $\Omega_1 = \Omega_{11} \cup \Omega_{12}$ :

$$a_1(\mathbf{u}_1, \mathbf{v}_1) = a_{11}(\mathbf{u}_1, \mathbf{v}_1) + a_{12}(\mathbf{u}_1, \mathbf{v}_1), \quad \forall \mathbf{u}_1 \in \mathcal{U}_1, \quad \forall \mathbf{v}_1 \in \mathcal{V}_1, \quad (16)$$

which leads to the following simplification of Eq. (15):

$$\begin{cases} \text{Find } \mathbf{u}_1 \in \mathcal{U}_1 \text{ such that:} \\ a_1(\mathbf{u}_1, \mathbf{v}_1) = l_{11}(\mathbf{v}_1) + a_{12}(\mathbf{u}_1, \mathbf{v}_1), \quad \forall \mathbf{v}_1 \in \mathcal{V}_1. \end{cases} \quad (17)$$

Finally, by writing the equilibrium of domain  $\Omega_{12}$ :

$$a_{12}(\mathbf{u}_1, \mathbf{v}_1) = l_{12}(\mathbf{v}_1) + \int_{\Gamma} \underline{\underline{\sigma}}_{12}(\mathbf{u}_1) \mathbf{n}_{12} \cdot \mathbf{v}_1 d\Gamma, \quad \forall \mathbf{v}_1 \in \mathcal{V}_1, \quad (18)$$

$\mathbf{n}_{12}$  being the outward unit normal to  $\Omega_{12}$  along  $\Gamma$  and  $\underline{\underline{\sigma}}_{12}$  being the Cauchy stress tensor associated to  $\Omega_{12}$ , the problem can be recast as:

$$\begin{cases} \text{Find } \mathbf{u}_1 \in \mathcal{U}_1 \text{ such that:} \\ a_1(\mathbf{u}_1, \mathbf{v}_1) = l_1(\mathbf{v}_1) + \int_{\Gamma} \underline{\underline{\sigma}}_{12}(\mathbf{u}_1) \mathbf{n}_{12} \cdot \mathbf{v}_1 d\Gamma, \quad \forall \mathbf{v}_1 \in \mathcal{V}_1. \end{cases} \quad (19)$$

For the resolution, a fixed point as in Eqs. (11) and (12) can be implemented. This time, only Neumann problems need to be solved. For the  $n^{\text{th}}$  iteration, we proceed as follows: starting with  $\mathbf{u}_1^{(0)} \in \mathcal{U}_1$ , we look for  $\mathbf{u}_1^{(n)} \in \mathcal{U}_1$  such that:

$$a_1(\mathbf{u}_1^{(n)}, \mathbf{v}_1) = l_1(\mathbf{v}_1) + \int_{\Gamma} \underline{\underline{\sigma}}_{12}(\mathbf{u}_1^{(n-1)}) \mathbf{n}_{12} \cdot \mathbf{v}_1 d\Gamma, \quad \forall \mathbf{v}_1 \in \mathcal{V}_1. \quad (20)$$

Thanks to the prolongation of the global model over  $\Omega_{12}$ , the global operators  $a_1$  and  $l_1$  over  $\Omega_1$  are now involved without any modification. During the iterations, only reaction forces across  $\Gamma$  need to be computed. In this sense, the strategy is said to be non-intrusive. In our case of a NURBS discretization, this may highly facilitate the modelling of geometric details since it avoids the complex task of constructing a new NURBS parametrization of the global model (and of re-constructing it each time the detail evolves).

### 3.2.2. The discrete version.

Let us introduce the NURBS functions  $(N_A^1)_{A \in \{1, 2, \dots, n^1\}}$  that discretize domain  $\Omega_1$ . Following the principle of isoparametric elements, the basis  $(N_A^1)_{A \in \{1, 2, \dots, n^1\}}$  is used to build the finite element space  $\mathcal{U}_1^h$  corresponding to the discretization of  $\mathcal{U}_1$ . By substituting this NURBS approximation in the weak form Eq. (19) and performing as in Eq. (20), we can derive the dis-

crete non-intrusive algorithm. For the  $n^{\text{th}}$  iteration, we proceed as follows: starting with  $\{U_1\}^{(0)}$ , we look for  $\{U_1\}^{(n)}$  such that:

$$[K_1] \{U_1\}^{(n)} = \{F_1\} + \{R_{12}\}^{(n-1)}. \quad (21)$$

Operator  $[K_1]$  (respectively  $\{F_1\}$ ) is the classical stiffness matrix (resp. vector force) associated to domain  $\Omega_1$  and,  $\{R_{12}\}$  is introduced to denote the discrete reaction forces at  $\Gamma$  of the global model in the fictitious part ( $\Omega_{12}$ ). The convergence test usually performed to stop this algorithm relies on the discrete equilibrium of the reaction forces of the initial coupled problem at the interface  $\Gamma$ . Since in this case domain  $\Omega_2$  is void, we simply need to verify that the reaction forces at  $\Gamma$  of the global model in  $\Omega_{11}$ , denoted  $\{R_{11}\}$ , are sufficiently close to zero. This leads to the following definition of the interface equilibrium residual:

$$\eta_{\text{void}} = \frac{\|\{R_{11}\}\|}{\|\{F_1\}\|}. \quad (22)$$

It may be noted that the fictitious prolongation of the global solution over  $\Omega_{12}$  has no physical meaning (it depends on the initialization). Moreover, it is important to notice that the algorithm proposed here is the standard one and that its convergence may be slow in certain situations. To answer this issue, acceleration techniques, such as based on an Aitken's Delta Squared method or a Quasi-Newton method, can be applied to the present situation from the existing developments in classical FEM (see, e.g., [30]). Numerical experiments to account for this point will be carried out in section 4.

**Remark 4.** *With its discrete version in hand (see Eq. (21)), the physics of the new problem may be easily understandable. Indeed, roughly speaking, the new problem to be solved is a problem over  $\Omega_1$  that is subjected along  $\Gamma$  to a surface force  $\{R_{12}\}$ . As a consequence, performing the equilibrium of the new problem at  $\Gamma$  leads to:*

$$\{R_{11}\} + \{R_{12}\} = \{R_{12}\} \quad \Rightarrow \quad \{R_{11}\} = \{0\}, \quad (23)$$

*which enables to recover that  $\Gamma$  constitutes a free boundary for the problem solved in  $\Omega_{11}$ .*

### 3.2.3. Implementation: computation of the interface reaction forces.

The setting up of algorithm (21) requires the evaluation of the reaction forces  $\{R_{12}\}$ . In order to be consistent with the discrete approximations,

$\{R_{12}\}$  has to be computed from its associated stiffness matrix and vector force as follows:

$$\{R_{12}\} = ([K_{12}] \{U_1\} - \{F_{12}\})|_{\Gamma}. \quad (24)$$

This implies performing a volume integral of the form:

$$a_{12} (\mathbf{u}_1^h, \mathbf{v}_1^h) + l_{12} (\mathbf{v}_1^h), \quad (25)$$

and applying the restriction operator  $\cdot|_{\Gamma}$  on a discrete vector. The restriction operator on  $\Gamma$  of a discrete vector  $\{F\}$  is defined such that:

$$\{F\}|_{\Gamma} = [B_{\Gamma}] \{F\}, \quad (26)$$

where  $[B_{\Gamma}]$  is the Boolean trace operator that selects only the degrees of freedom concerned by the interface.

**Remark 5.** *We emphasize that the computation of the reaction forces from a volume integral and not directly from a surface integral (as in Eq. (19)) is necessary to obtain a non-intrusive strategy in the discrete case as the finite element error is not taken into account otherwise. We specify that in the finite element setting, Eq. (18) becomes :*

$$[K_{12}] \{U_1\} = \{F_{12}\} + ([K_{12}] \{U_1\} - \{F_{12}\})|_{\Gamma}. \quad (27)$$

*Such a decomposition is usual in FEM non-intrusive coupling (see, e.g., [11, 29, 30]).*

Although implementing the volume integral (24)- (25) is quite straightforward in FEM, the extension in the NURBS context may require additional attention. Conforming geometries are usually considered in FEM (see, e.g., [12, 11, 30]) whereas, due to the rigid tensor product structure of NURBS, non-conforming geometries need to be addressed in this work (there is no reason for the interface  $\Gamma$  to be aligned with the edges of the elements in  $\Omega_1$ ). To perform the calculation (24), a special integration scheme is required to evaluate the contribution of the global operators in  $\Omega_{12}$  only. We recall that the only available data regarding  $\Omega_2$  is the parametrization of the trimming curve that forms its boundary  $\partial\Omega_2$ . For the general case, existing techniques could be used to define a suitable quadrature rule: for instance, the standard sub-triangulation technique in the context of X-FEM [42], or the hierarchical element subdivision employed in the FCM [25, 19, 20], or

the technique used in the NURBS Enhanced FEM [43]. Now, for most cases arising in the situation of geometric details, it seems that an exact NURBS domain may be simply constructed from the NURBS trimming curve by adding multiple interpolatory control points at the center of the detail.

To illustrate the strategy, we return to the example of Fig. 1, namely a plate with a circular hole. The basis of our strategy is to construct a NURBS parametrization of the surface contained inside the circular curve (in red in Fig.1). Let us denote this surface ( $\Omega_{12}$ ) by the disk and its boundary ( $\Gamma$ ) by the circular curve. To generate the disk with NURBS, as many control points as necessary to define the circular curve (with the same weights as for the curve) can be put and matched together at the center of the circular curve. The initial NURBS parametrization of the disk is composed of four elements of degree two in the circumferential direction and of degree one in the radial direction (see Fig. 5(a)). Then, usual NURBS mesh refinement techniques can be applied to produce a quadrature rule enabling the behaviour of the global model to be accurately seized in the disk  $\Omega_{12}$  (see Fig. 5(b) for a mesh of 8 (circumferential direction)  $\times$  2 (radial direction) elements with a  $3 \times 3$  Gaussian rule per element). From the newly constructed NURBS parametrization of the disk, the standard integration rule for NURBS is used:  $p + 1$  Gauss points ( $p$  being the polynomial order) are considered in each direction per element. The last thing to be done is to pull back the quadrature points to the parametric domain of the plate (see Fig. 5(c)). This can be achieved simply by performing Newton-Raphson iterations to inverse the NURBS mapping:

$$\mathbf{x}_i^{\text{gauss}} = \sum_{A=1}^{n_1} N_A^1(\boldsymbol{\xi}_i^{\text{gauss}}) \mathbf{x}_A^1 \quad \Rightarrow \quad \boldsymbol{\xi}_i^{\text{gauss}}. \quad (28)$$

$\mathbf{x}_i^{\text{gauss}}$  denotes the coordinates of the quadrature points in the physical space and  $\boldsymbol{\xi}_i^{\text{gauss}}$  refers to the corresponding coordinates in the parametric space. The advantage of the proposed technique is that it produces NURBS conforming quadrature rules simply (in the sense that the quadrature points are aligned with the trimming curve that bounds the NURBS domain). Such a strategy applies directly to all types of star domains. Based on the same principle, we believe that most of the details of engineering interest can be generated with a few additional efforts. Corresponding investigations are in progress to generalize the procedure. We also note that new strategies producing conforming quadrature rules for trimmed surfaces have appeared

very recently (see Nagy *et al.* [44] and Kudela *et al.* [45]) and may constitute promising options to be considered in our future works.

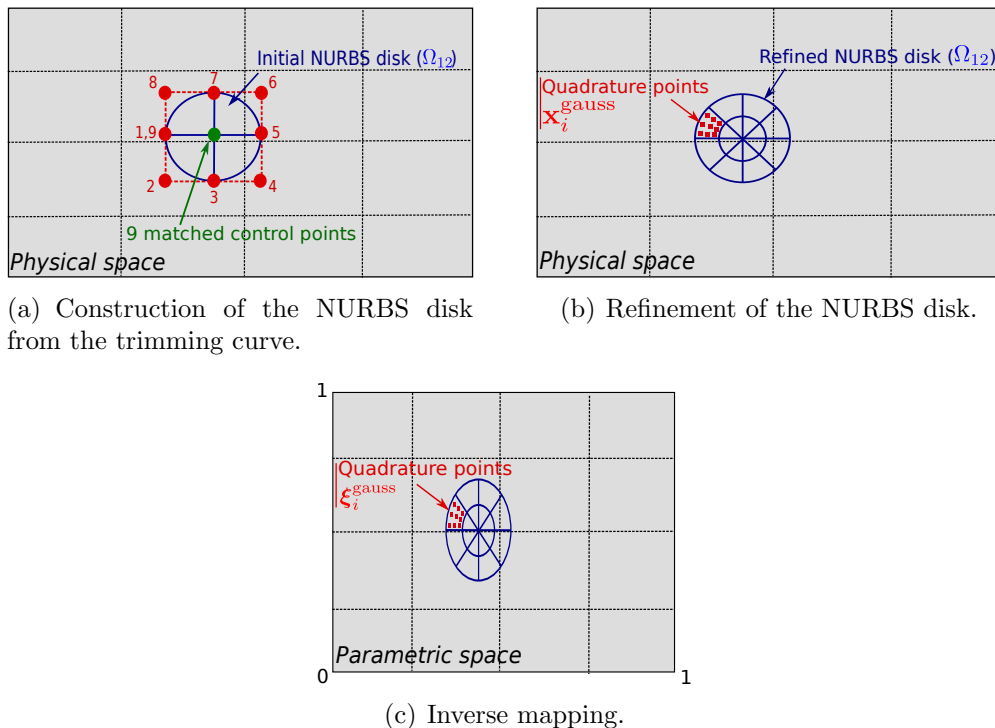


Figure 5: Construction of a suitable quadrature rule for  $\{R_{12}\}$ .

**Remark 6.** We emphasize that the NURBS mesh of Fig. 5(b) is only constructed here to produce an accurate integration rule for  $[K_{12}]$  and  $\{F_{12}\}$ . The corresponding stiffness operator is never assembled and factorized. Furthermore, it may be noted that operators  $[K_{12}]$  and  $\{F_{12}\}$  are of small size (the NURBS function  $N_A^1$ , whose support does not reach the small region  $\Omega_{12}$ , does not contribute), and can be computed in the pre-processing step. As a result, the computation of the reaction forces only requires small-size matrix-vector products during the non-intrusive algorithm, which is not expensive.

**Remark 7.** With the above developments, the problem can be solved directly by performing:

$$([K_1] - [K_{12}]) \{U_1\} = \{F_1\} - \{F_{12}\}. \quad (29)$$

In this sense, the method can be classified as a fictitious domain approach and is very close to the so-called NURBS FCM [25, 19, 20], the only difference being the quadrature rule used. Rather than computing Eq. (29), we believe that the proposed non-intrusive strategy (Eq. (21)) may be more suitable for the modelling of geometric details that could evolve during the simulation. Independently of the shape of the geometric details, the global stiffness operator is assembled and factorized only once and the system to be solved remains well-conditioned. The price to pay is the number of iterations, but this can be strongly reduced by means of acceleration techniques.

**Remark 8.** Setting up the non-intrusive algorithm (21) also requires computation of the reaction forces  $\{R_{11}\}$  to evaluate the equilibrium residual (22). This is obtained from the already-computed stiffness  $[K_{12}]$  and force  $\{F_{12}\}$  as follows:

$$\{R_{11}\} = (([K_1] - [K_{12}]) \{U_1\} - (\{F_1\} - \{F_{12}\}))|_{\Gamma}. \quad (30)$$

### 3.3. Part 2: Case of "covered" local models

#### 3.3.1. The continuum version.

The strategy proposed for geometric details can easily be extended to the modelling of covered local behaviours in a NURBS patch (*i.e.*, when  $\Omega_2$  is not void but constitutes a real domain, see Fig. 4(b)). Indeed, going back to the reference problem of section 2.2, exactly the same procedure as for a void local model can be applied to Eq. (11) to rewrite the Neumann problem over the whole NURBS patch  $\Omega_1$ . By doing that, the global/local non-intrusive algorithm straightforwardly follows from the standard algorithm (11)-(12). For the  $n^{\text{th}}$  iteration, we start with  $\mathbf{u}_1^{(0)} \in \mathcal{U}_1$  and  $\boldsymbol{\lambda}^{(0)} \in \mathcal{M}$  and we look for  $\mathbf{u}_1^{(n)} \in \mathcal{U}_1$ ,  $\mathbf{u}_2^{(n)} \in \mathcal{U}_2$ , and  $\boldsymbol{\lambda}^{(n)} \in \mathcal{M}$  such that:

1. Resolution of a Neumann problem over  $\Omega_1$ :

$$a_1(\mathbf{u}_1^{(n)}, \mathbf{v}_1) = l_1(\mathbf{v}_1) - b(\boldsymbol{\lambda}^{(n-1)}, \mathbf{v}_1) + \int_{\Gamma} \underline{\underline{\sigma}}_{12}(\mathbf{u}_1^{(n-1)}) \mathbf{n}_{12} \cdot \mathbf{v}_1 d\Gamma, \quad \forall \mathbf{v}_1 \in \mathcal{V}_1. \quad (31)$$

2. Resolution of a Dirichlet problem over  $\Omega_2$ :

$$\begin{cases} a_2(\mathbf{u}_2^{(n)}, \mathbf{v}_2) - b(\boldsymbol{\lambda}^{(n)}, \mathbf{v}_2) = l_2(\mathbf{v}_2), & \forall \mathbf{v}_2 \in \mathcal{V}_2; \\ b(\boldsymbol{\mu}, \mathbf{u}_2^{(n)}) = b(\boldsymbol{\mu}, \mathbf{u}_1^{(n)}), & \forall \boldsymbol{\mu} \in \mathcal{M}. \end{cases} \quad (32)$$

Once again, the operators over the whole global NURBS patch are now involved in Eq. (31) without any modification and, only displacement and force exchanges at the interface  $\Gamma$  are required. This accounts for the non-intrusiveness of the strategy and thus, for the simplicity of the method to model local behaviours in a NURBS patch.

### 3.3.2. The discrete version.

To derive the discrete version of the global/local non-intrusive algorithm (31)-(32), we need to introduce the approximation spaces  $\mathcal{U}_2^h$  and  $\mathcal{M}^h$  associated to  $\mathcal{U}_2$  and  $\mathcal{M}$ , respectively. Keeping the principle of isoparametric element, we consider for  $\mathcal{U}_2^h$  the basis functions  $(N_B^2)_{B \in \{1,2,\dots,n^2\}}$  that discretize domain  $\Omega_2$ . For the discretization of the Lagrange multiplier space, special care may be required since bad-chosen basis can lead to undesirable energy-free oscillations (due to the non-satisfaction of the *inf-sup* condition). For the sake of simplicity, we adopt in this work a classical strategy (see, *e.g.*, [30]): the trace along the coupling interface  $\Gamma$  of the basis functions of domain  $\Omega_2$  is considered for  $\mathcal{M}^h$ . With such a choice, we never encountered instabilities in our computations. The discrete version can then be written as follows: for the  $n^{\text{th}}$  iteration, we start with  $\{U_1\}^{(0)}$  and  $\{\Lambda\}^{(0)}$  and we look for  $\{U_1\}^{(n)}$ ,  $\{U_2\}^{(n)}$ , and  $\{\Lambda\}^{(n)}$  such that:

1. Resolution of a Neumann problem over  $\Omega_1$ :

$$[K_1] \{U_1\}^{(n)} = \{F_1\} - [C_1]^T \{\Lambda\}^{(n-1)} + \{R_{12}\}^{(n-1)}. \quad (33)$$

2. Resolution of a Dirichlet problem over  $\Omega_2$ :

$$\begin{bmatrix} [K_2] & -[C_2]^T \\ -[C_2] & [0] \end{bmatrix} \begin{Bmatrix} \{U_2\}^{(n)} \\ \{\Lambda\}^{(n)} \end{Bmatrix} = \begin{Bmatrix} \{F_2\} \\ -[C_1] \{U_1\}^{(n)} \end{Bmatrix}. \quad (34)$$

$[C_1]$  and  $[C_2]$  are the classical mortar coupling operators. To stop the algorithm, the global reaction forces at  $\Gamma$  ( $\{R_{11}\}$ ) have to be compared to the local reaction forces pulled back in  $\Omega_{11}$ , *i.e.*  $\{R_2\} = [C_1]^T \{\Lambda\}$ . It leads to the following equilibrium residual:

$$\eta_{\text{covered}} = \frac{\|\{R_{11}\} + \{R_2\}\|}{\|\{F_1\}\|}. \quad (35)$$

We emphasize that such an algorithm is classical in non-intrusive coupling and has been widely studied in the field of FEM. For more information, the interested reader is advised to consult Duval *et al.* [30] and references cited therein. Finally, the same remarks as for a void local model can be done about the algorithm. The fictitious prolongation of the global solution over  $\Omega_{12}$  has no physical meaning and has to be replaced by the solution in  $\Omega_2$ . The number of iterations of the algorithm can be reduced by means of Aitken or Quasi-Newton acceleration techniques.

### 3.3.3. Implementation aspects.

Since in this case the discretization of domain  $\Omega_2$  is explicitly known, we use it to simply compute the quadrature rule required to evaluate the reaction forces  $\{R_{12}\}$  of  $\Omega_{12}$  (and so  $\{R_{11}\}$ , see remark 8). As well, we use the integration rule coming from the discretization of the part  $\Gamma$  of the boundary  $\partial\Omega_2$  for the computation of the coupling matrices  $[C_1]$  and  $[C_2]$ . Since the global and local problems are solved alternatively in a non-intrusive strategy, two different numerical codes can be used for the resolution (one for the global Neumann problem (33) and the other for the local Dirichlet problem (34)). This feature offers an important flexibility to the method. Indeed, if a linear NURBS code is used for the global NURBS problem, any other existing robust codes (NURBS, FEM, X-FEM, FCM) suitable for the modelling of complex behaviours (fracture, plasticity, contact) may be used to incorporate an accurate local model. The only need for that is to be able to apply Dirichlet boundary conditions to the local problem and to extract from its resolution the reaction forces at  $\Gamma$  and the quadrature rules in  $\Omega_2$  and over  $\Gamma$  (see Fig. 6 for illustration). The local model actually acts as a correction applied to the global model on the right-hand side.

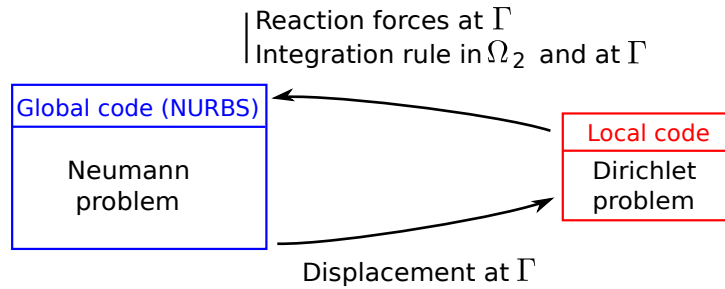


Figure 6: The non-intrusive strategy: coupling of codes.

## 4. Numerical results

We now present a range of numerical examples in two-dimensional linear elasticity in order to assess the performance of the proposed strategy. As in the previous section, the presentation is divided into two parts: first, the situation of a "void" local model is addressed in section 4.1; then, the more usual case of enrichment by a "covered" local model is investigated in section 4.2. We recall that the local model is said to be "void" when the associated region constitutes a hole, while the adjective "covered" is used to qualify a local model over the existing real region  $\Omega_2$ . Regarding the discretization of the global model, we start from a patch composed of a single element, to which we apply the  $k$ -refinement strategy. Thus, the continuity across the interior knots is  $C^{p-1}$ ,  $p$  being the polynomial degree of the NURBS functions. From here on, the mesh composed of  $N$  elements along the first length and  $M$  elements along the second length will be denoted  $N \times M$ . In the illustrations, we keep the notations introduced in the previous section; in particular, domain  $\Omega_1 = \Omega_{11} \cup \Omega_{12}$  characterizes the global NURBS patch, the model of which in domain  $\Omega_{12}$  is to be replaced either by a void model or by another discrete model contained in domain  $\Omega_2$ .

### 4.1. Modelling of geometric details

In this first part, the methodology implemented is the one related to section 3.2. Our interest here is in how geometric details are modelled. Two numerical examples are investigated. In the first one, where an analytical reference solution is available, we illustrate that our non-intrusive methodology does not compromise accuracy and that few iterations are required, especially when acceleration techniques are used. In the second example, we illustrate the potential of the method to treat more complex cases of geometric details.

#### 4.1.1. Infinite plate with a circular hole.

**Description of the test case:** To start with, the popular example of an infinite plate with a circular hole under in-plane tension is considered. The geometry, material, boundary conditions and the analytical solution [46] are given in Fig. 7. Because of symmetry, the problem is restricted to one quarter of the plate. This problem was among the first to be studied with NURBS [1, 2] and was later investigated in the framework of the fictitious domain concept [14]. The discretization of the problem following the non-intrusive strategy developed is illustrated in Fig. 8(a). A regular B-Spline

mesh is used for the plate without the hole (domain  $\Omega_1$ ) and a circular NURBS mesh is constructed to produce a suitable quadrature rule in the fictitious domain  $\Omega_{12}$ . Again, we emphasize that the only aim of this circular mesh is the derivation of the quadrature rule: the associated stiffness operator is never assembled and factorized. For a curved domain, the first length (where there are  $N$  elements) is the circumferential length and the second length (discretized by  $M$  elements) is the radial length. This notation also holds for the following examples.

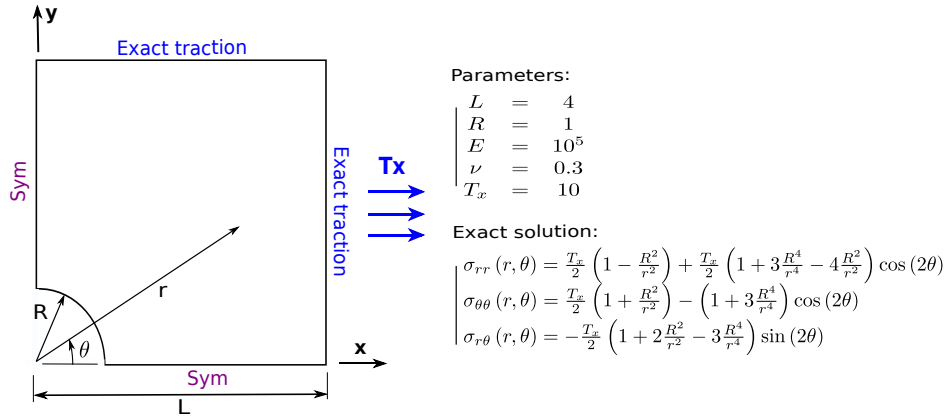
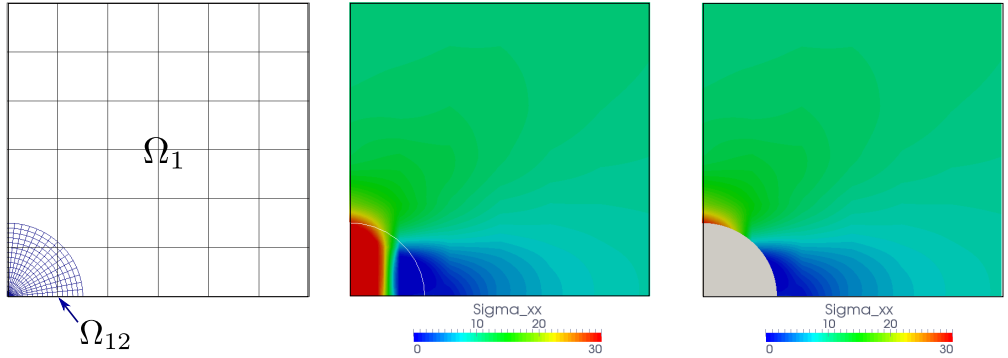


Figure 7: Infinite plate with a circular hole: description and data of the problem.

**Study of the non-intrusive algorithm:** First, the behaviour of the non-intrusive algorithm (21) is studied. The results obtained with the discretization of Fig. 8(a) are grouped in Figs. 8(b)-8(e). More precisely, Figs. 8(b) and 8(c) show plots of the normal stress in the horizontal  $x$ -direction obtained (once the algorithm has converged) in the embedded domain  $\Omega_1$  and in the true domain  $\Omega_{11}$ , respectively. Removing the smooth non-physical fictitious prolongation in  $\Omega_{12}$ , the solution appears to be in good agreement with references [1, 2, 14]. Figs. 8(b) and 8(c) enable the convergence of the iterative algorithm to be appreciated: first, in terms of the equilibrium residual (Eq. (22)) and then in terms of the error on the displacements in energy norm. Note that the error is computed by taking only contributions in  $\Omega_{11}$  into account. The standard fixed point and also Aitken's Delta squared and Quasi-Newton acceleration techniques are implemented. The equilibrium residual falls to zero, which accounts for the convergence of the algorithm. Conversely, the error on the displacement reaches an asymptotic

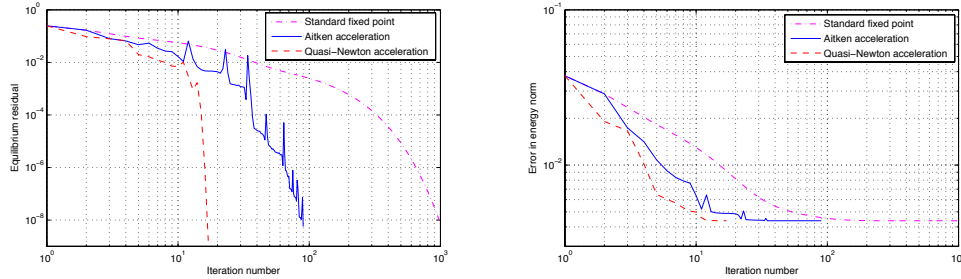
value, which corresponds to the NURBS finite element approximation. As noted in remark 7, the use of acceleration techniques strongly reduces the number of iterations: the number of iterations needed to attain the finite element accuracy, which seems to be obtained for a residual of about  $10^{-3}$ , is reduced by a factor of ten in this example.



(a) Mesh (black) and support of the quadrature rule (blue).

(b) Normal stress  $\sigma_{xx}$  plotted over  $\Omega_1$ .

(c) Normal stress  $\sigma_{xx}$  plotted over  $\Omega_{11}$ .



(d) Convergence of the interface equilibrium residual.

(e) Convergence of the displacements in the energy norm.

Figure 8: Non-intrusive analysis of the infinite plate with a circular hole (rectangular B-spline mesh of quadratic  $6 \times 6$  elements for  $\Omega_1$  + circular NURBS mesh of quadratic  $15 \times 15$  elements for the quadrature rule in  $\Omega_{12}$ ).

**Remark 9.** *By comparing Figs. 8(d) and 8(e), it may be noted that reaching a residual as low as  $10^{-8}$  is probably not necessary to achieve an accurate numerical solution. Nevertheless, as the development of efficient convergence criteria was not the purpose of the present contribution, we kept a value of*

$10^{-8}$  for the equilibrium residual to stop the algorithm. Thus the number of iterations required is probably overestimated.

**Study of the finite element convergence:** Then, the convergence of the method with respect to the mesh size is studied. Here, the non-intrusive algorithm is performed until convergence. To get a general view, Fig. 9 shows plots of the normal stress in the horizontal  $x$ -direction for different cubic B-spline meshes of the global patch, which can be directly compared to corresponding plots given in [14]. No visible difference with [14] can be observed. To go further, the convergence behaviour of the displacements in the energy norm under uniform refinement is plotted in Fig. 10, starting from a mesh of  $4 \times 4$  B-spline elements for the global model. Polynomial degrees  $p = 1$ ,  $p = 2$  and  $p = 3$  are considered in both spatial directions. We note that the NURBS mesh of the hole needs to be sufficiently fine to give a suitable quadrature rule for the interface reaction forces. We use a NURBS mesh composed of  $50 \times 50$  elements for the finer B-spline mesh of the global model. The optimal rates of convergence of  $h^p$  are seen to be achieved ( $h$  being the characteristic element size), which demonstrates that the methodology does not interfere with the accuracy of the NURBS functions.

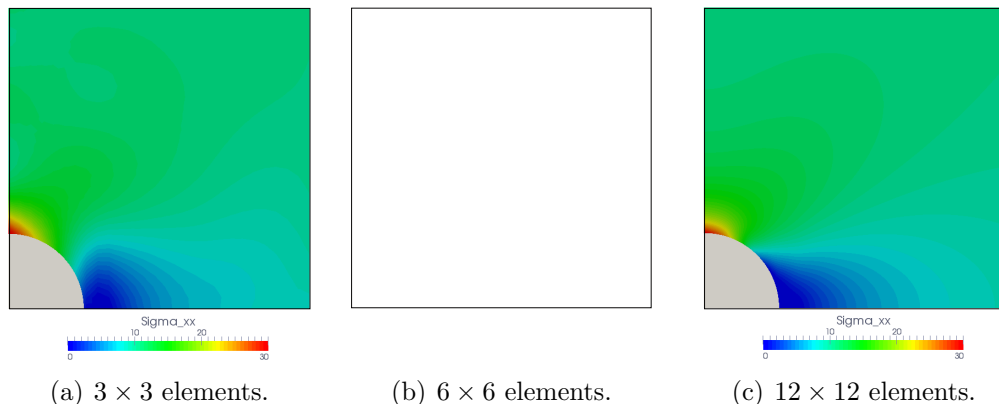


Figure 9: Normal stress  $\sigma_{xx}$ , plotted over  $\Omega_{11}$ , for different cubic B-spline meshes.

#### 4.1.2. Perforated strip under tension.

**Description of the test case:** To illustrate the robustness of the method, the more complex case of a plane strip perforated in its middle

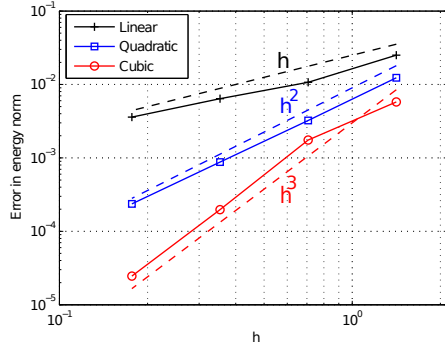
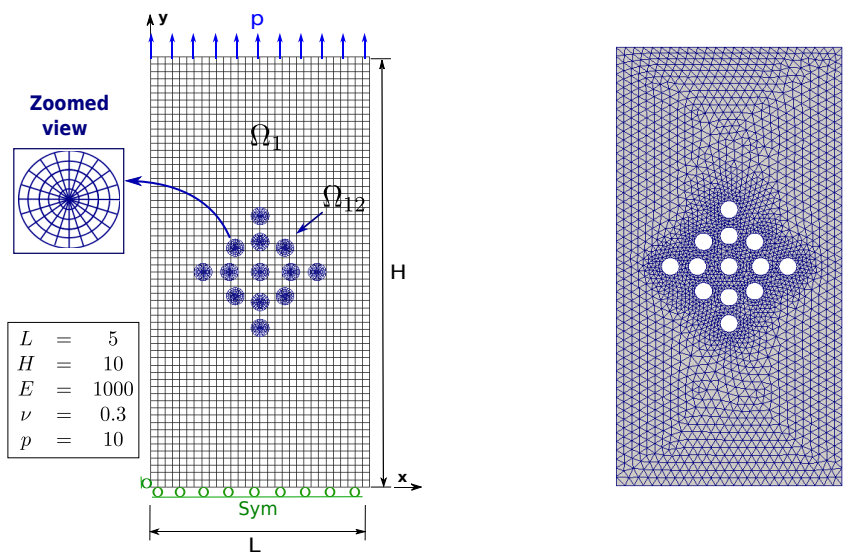


Figure 10: Convergence of the displacement in the energy norm, when the B-spline grid is uniformly refined.

part by several holes and subjected to constant in-plane tension is now computed. The numerical model is described in Fig. 11(a). Note that such a test case is usually encountered in the field of immersed boundary methods (see, *e.g.*, [19]). In our non-intrusive model, a regular quadratic B-spline mesh is used for the global model of the plate without the holes and each hole is specified by a circular NURBS mesh. We emphasize that the interest of the method here is the simplicity with which it handles a modification of the perforation (size and number of holes). For comparison purposes, a refined finite element solution is computed using the classical linear triangular elements implemented in Code\_Aster [47]. The corresponding boundary fitted discretization is shown in Fig. 11(b).

**Numerical results:** The results are given in Fig. 12. Figs. 12(a)-12(c) show, respectively, the displacement in the  $x$ -direction, the displacement in the  $y$ -direction and the von Mises stress obtained with the non-intrusive model of Fig. 11(a). The same information is plotted in Figs. 12(d)-12(f) for the reference FE solution. The two solutions are very close, which shows the accuracy of the non-intrusive methodology. The horizontal and vertical displacements exhibit a necking effect due to the stiffness reduction induced by the perforations and the typical stress concentration phenomena around the holes are well represented. Finally, the convergence of the non-intrusive algorithm can be observed in Fig. 12(g): a residual of  $10^{-4}$  is obtained in about 20 iterations and approximately 30 iterations are required to reach a residual of  $10^{-8}$ .



(a) NURBS non-intrusive problem (rectangular B-spline mesh of quadratic  $30 \times 60$  elements for  $\Omega_1$  + 13 circular NURBS meshes of quadratic  $20 \times 5$  elements for the quadrature rule in  $\Omega_{12}$ ).

(b) Reference linear triangular mesh (from Code\_Aster).

Figure 11: Perforated tensile specimen.

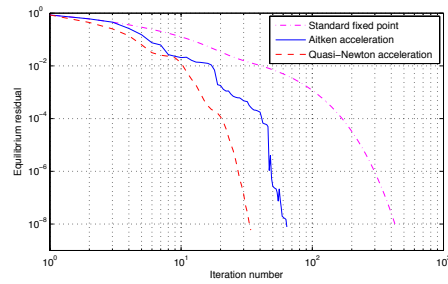
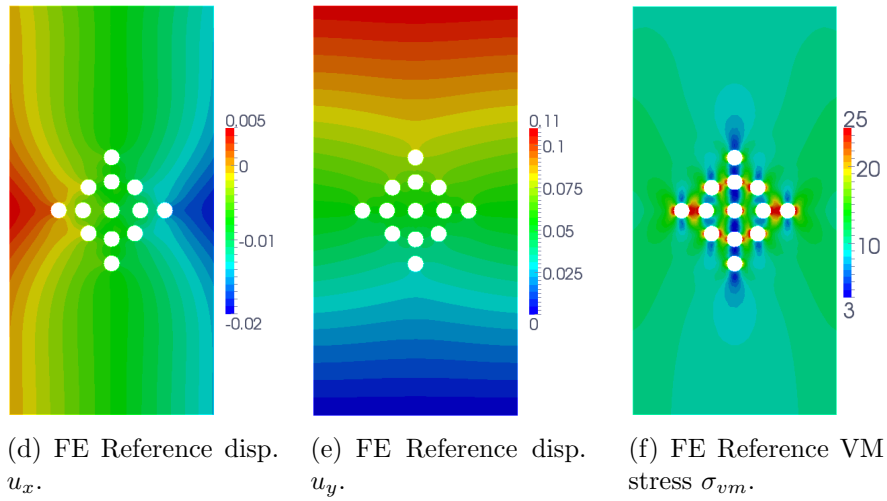
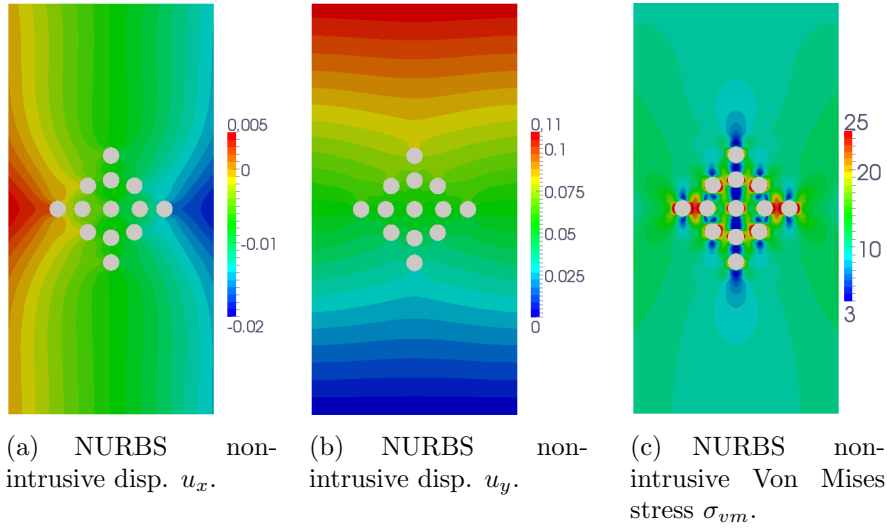


Figure 12: Non-intrusive analysis of the perforated strip under tension and comparison with a reference FE solution.

## 4.2. Modelling of local behaviours

In this second part, we illustrate the behaviour of the proposed non-intrusive strategy when applied to covered local models. The developments established in section 3.3 are implemented here and three examples are considered. In the first, the strategy is used to perform NURBS local refinement on a simple test case, which demonstrates that the non-intrusive coupling method does not compromise accuracy. The second example concerns applications to micromechanics of materials. In particular, the ability of the method to treat a plate with a stiffer inclusion is shown. Finally, the non-intrusive coupling of two different types of elements (NURBS and FEM) coming from two different numerical codes is performed to model a crack in a NURBS patch.

### 4.2.1. Curved beam subjected to end shear.

**Description of the test case:** The first example consists of a curved beam subjected to end shear. The problem, together with its non-intrusive discretization, is illustrated in Fig. 13(a). A constant radial displacement of  $u_0 = 0.01$  units is prescribed over the lower beam boundary. An analytical solution for a reference plane stress model is available for the problem in [48]. The same polynomial order is used in both spatial directions and for the global model as well as for the local model. A minimum order of  $p = 2$  is necessary to represent the curvature exactly. In the upper half of the structure, the global NURBS model is meant to be replaced by a more refined (along the radial direction) NURBS model. We posit that the material properties are the same for the global and local models, the only difference being the mesh size. In order to address the coupling of non-conforming geometries, an odd number of elements along the circumferential direction is considered for the global patch. Such a choice leads to an interface  $\Gamma$  that cuts (in the middle) a layer of elements of the global model.

#### Numerical results:

- The results obtained (once the non-intrusive algorithm has converged) with the discretization of Fig. 13(a) are shown in terms of displacement in Fig. 13(b) and in terms of Von Mises stress in Figs. 13(c) and 13(d). The Von Mises error is normalized by the maximum reference Von Mises stress encountered in the domain. We emphasize that it is the coupling solution in  $\Omega_{11} \cup \Omega_2$  that is mapped (the fictitious prolongation of the

global solution over  $\Omega_{12}$  is not represented). The solution corresponds to reference [48] (error of the Von Mises stress less than 0.4%, see Fig. 13(d)). In particular, there is no visible error concentration around the coupling interface  $\Gamma$ .

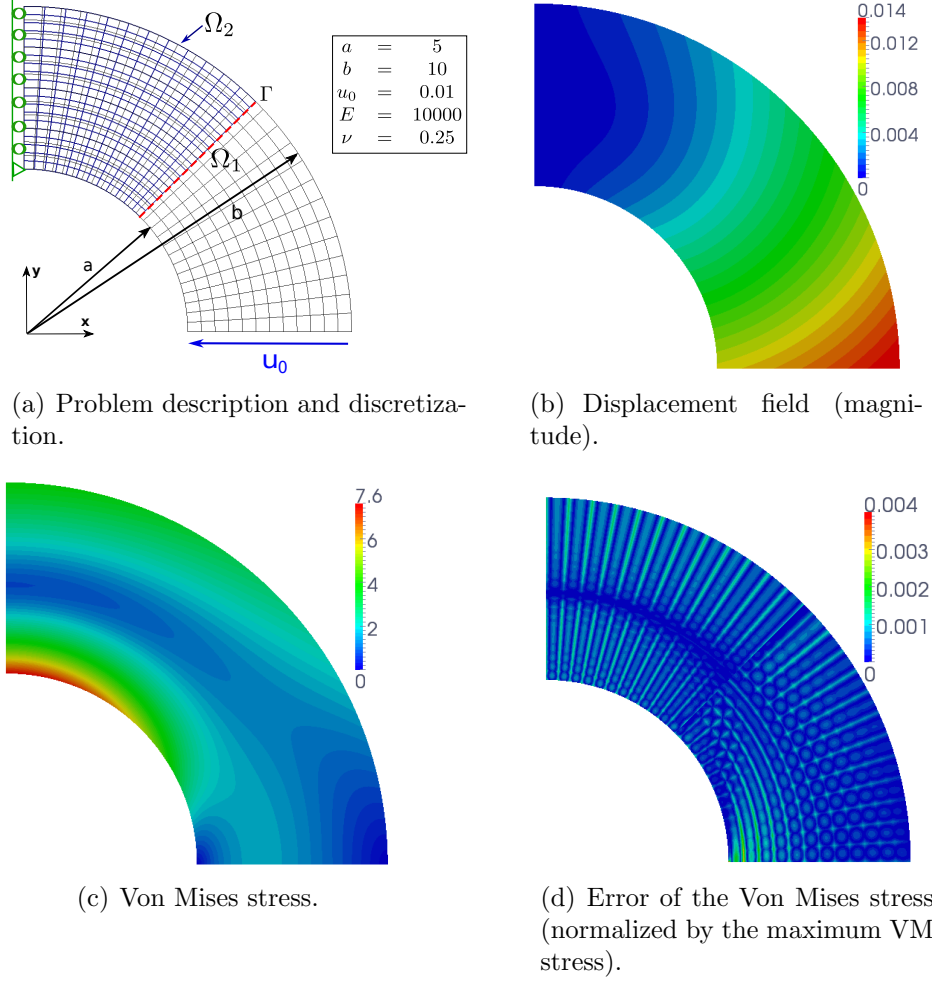


Figure 13: Non-intrusive analysis of the curved beam problem (NURBS mesh of quadratic  $25 \times 12$  elements for  $\Omega_1$  ( $12.5 \times 12$  elements for  $\Omega_{11}$ ) + NURBS mesh of quadratic  $12 \times 20$  elements for  $\Omega_2$ ).

- To better appreciate the accuracy of the method, we study the convergence of the coupling solution with the refinement of the mesh (see

Fig. 14). We proceed in the same way as in reference [48]: the convergence behaviour of the strain energy is considered. The relative energy error is computed as:

$$\frac{|E_d^{ex} - E_d^{fe}|}{E_d^{ex}}, \quad (36)$$

where  $E_d^{ex}$  denotes the reference exact strain energy and  $E_d^{fe}$  the strain energy of the NURBS finite element model. Orders  $p = 2$  and  $3$  are investigated. To refine the non-intrusive coupling solution, we consider the meshes indicated in Tab. 1 (right column). For each approximation, the first mesh discretizes domain  $\Omega_{11}$  (this is the global mesh divided in half along the circumferential direction; that is why half of the elements are involved) and the second mesh is used for domain  $\Omega_2$  (this is the local mesh). We note that the refinement obtained between successive meshes is not exactly uniform since there are always some elements of the global model that are cut. For comparison purposes, the convergence curves of (almost) equivalent single-patch solutions have been added in Fig. 14. Also, the equivalent single-patch meshes are reported in Tab. 1 (middle column). Finally, the convergence curves are plotted with respect to the equivalent number of elements  $N^{el}$  normalized by the number of elements  $N_1^{el}$  of the equivalent coarsest mesh (see left column of Tab. 1 for the associated values).

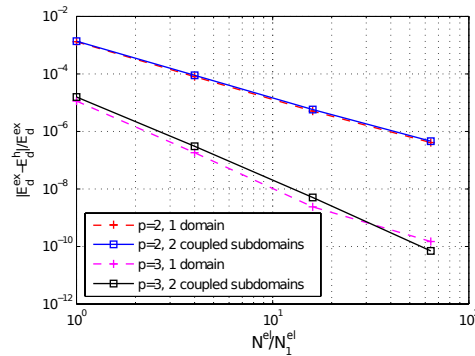


Figure 14: Convergence of the strain energy for uniform refinement in both subdomains.

- We observe that the rate of convergence and the error constant of the non-intrusive coupled discretizations are equivalent to those of the equivalent single-patch discretization. True, a slight discrepancy ap-

| Number of elements<br>( $N^{el}$ ) | Single-patch<br>mesh | Coupled discretization<br>( $\Omega_{11} \cup \Omega_2$ ) |
|------------------------------------|----------------------|---|
| 24 ( $= N_1^{el}$ )                | $6 \times 4$         | $3.5 \times 3 \cup 3 \times 5$                            |
| 96                                 | $12 \times 8$        | $6.5 \times 6 \cup 6 \times 10$                           |
| 384                                | $24 \times 16$       | $12.5 \times 12 \cup 12 \times 20$                        |
| 1536                               | $32 \times 48$       | $24.5 \times 24 \cup 24 \times 40$                        |

Table 1: Meshes considered to study the convergence behaviour.

pears since the single-patch model cannot exactly represent the non-conforming coupled model. For the finest cubic single-patch mesh, the error level is so low that it may be deteriorated by rounding errors. These results indicate that the error coming from the non-intrusive coupling methodology is significantly smaller than the error due to the NURBS finite element approximation. This means that the accuracy of NURBS is preserved with the proposed methodology when applied to covered local models.

#### 4.2.2. Plate with a central inclusion.

**Description of the test case:** With the next example, the situation of a non-conforming covered local model that has different material properties from those of the global model is investigated, considering the modelling of a plate with a central inclusion subjected to constant in-plane tension (see Fig. 15). Note that such types of test cases have already been computed using an embedded Nitsche’s method (see, *e.g.*, [9]). Here, the proposed non-intrusive coupling strategy is implemented. In order to be different from the situation of holes (where, roughly speaking, the local stiffness equals zero) and to be consistent with composite materials, the Young’s modulus is chosen to be a hundred times larger for the inclusion than for the plate ( $E_i = 100 \times E_p$ ). The Poisson’s coefficients are the same.

**Numerical models considered:** Two different numerical non-intrusive models are considered for the problem (see Fig. 15(a) for the first model and Fig. 15(b) for the second one). For each, a regular quadratic B-Spline grid is used for the global model and a circular quadratic NURBS mesh is constructed for the local model. However, in the first situation, the local model includes the inclusion only, while in the second case, an annulus of two elements in the radial direction is added at the boundary of the inclu-

sion to constitute the local model. In the second local model, two different materials separated by a  $C^0$  continuity then need to be considered to recover the solution of the initial problem:  $E_i$  is taken at the centre (*i.e.*, in the inclusion) and  $E_p$  is fixed in the annulus. By doing this, we will see that we are able to achieve good accuracy with relatively coarse meshes for the plate. The transition of the solution from the local model to the global one across  $\Gamma$  becomes smoother in the second situation while sharp phenomena need to be correctly captured in the first model. The difference of mesh size in the plate to obtain an equivalent solution with the first model and the second model is illustrated and reported in Fig. 15.

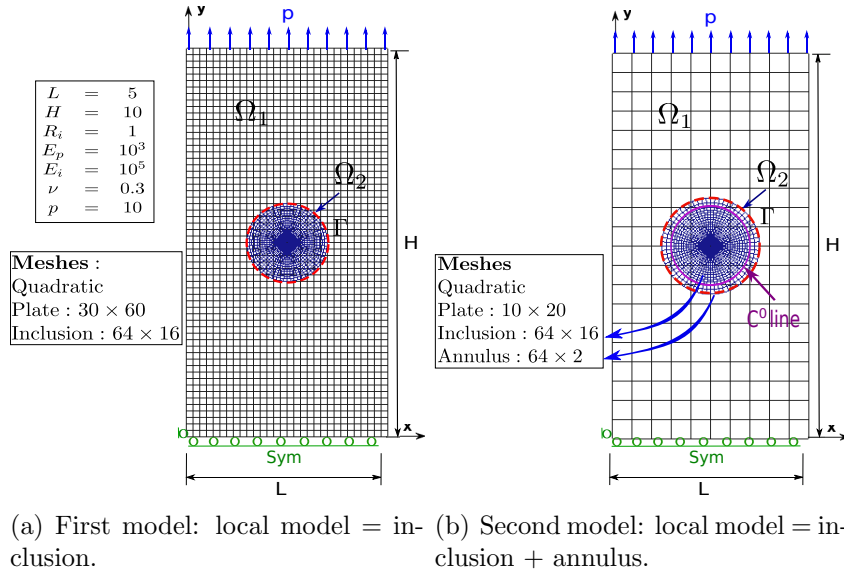


Figure 15: Plate with a central inclusion: description and discretization of the problem.

### Numerical results:

- The results obtained once the non-intrusive algorithm has converged are given in Figs. 16(a)-16(c) for the first model and Figs. 16(d)-16(f) for the second situation. The first plots are related to the discretization of Fig. 15(a) and the second plots concern the discretization of Fig. 15(b). For both models, the vertical displacement, the vertical strain and the Von Mises stress are shown. The solutions of the two models are in good agreement. The stiffer behaviour of the inclusion seems to be

well captured: the vertical strain is low while the Von Mises stress is high in the inclusion.

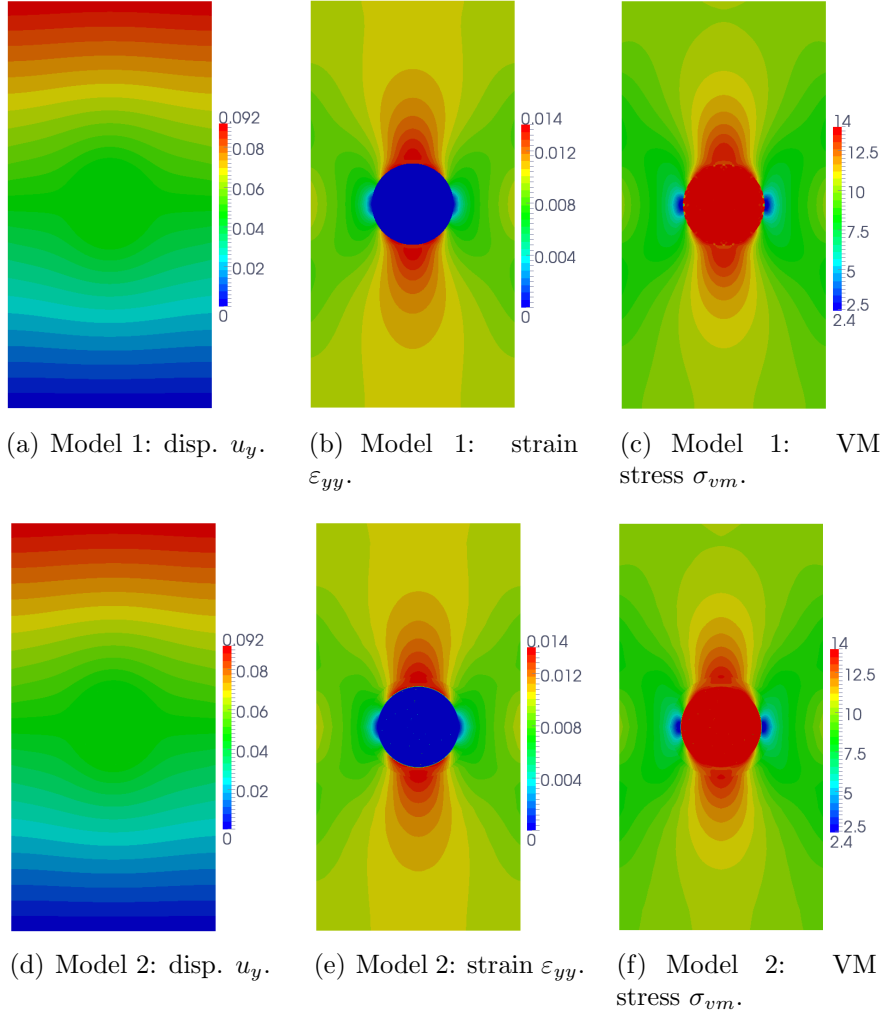
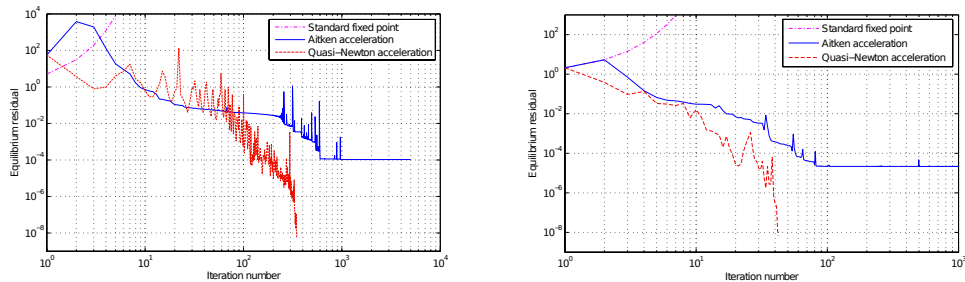


Figure 16: Plate with a central inclusion: converged solution of the non-intrusive analysis (top: first model, bottom: second model).

- The associated convergence behaviour of the non-intrusive algorithm is given in Fig. 17. As already observed in the framework of non-intrusive coupling in FEM, the Newton acceleration technique appears to be necessary to reach convergence in the situation of a local model

stiffer than the global model. Furthermore, we observe that the convergence is much slower for the first model (see Fig. 17(a)) than for the second model (see Fig. 17(b)) where the usual number of several tens of iterations is reached. The reason for this is the difference of stiffness between the global (fictitious) model in  $\Omega_{12}$  and the local model in  $\Omega_2$ . Theoretically, this can be shown by rewriting the fixed point as a modified Newton algorithm where the approximation of the tangent matrix depends on the gap in the primal Schur complements between the models in  $\Omega_{12}$  and in  $\Omega_2$  (see, *e.g.*, [30]). To conclude on these results, the two non-intrusive models implemented enable the problem to be solved accurately. Nevertheless, we emphasize that, for better convergence of the algorithm, the primal Schur complement of the local model (Dirichlet problem with prescribed displacement on  $\Gamma$ ) has to be relatively close to the primal Schur complement of the global model in  $\Omega_{12}$ . This is consistent with the original idea of global/local non-intrusive coupling: the region of the local model is expected to be sufficiently large to include both the small zone where complex behaviours are to be modelled (at its center) and larger regions (at its boundaries) where the connection with a simpler global model can be made efficiently.



(a) First model: interface equilibrium residual. (b) Second model: interface equilibrium residual.

Figure 17: Convergence of the non-intrusive algorithm for the plate with a central inclusion.

#### 4.2.3. Edge-cracked plate under uniaxial tension.

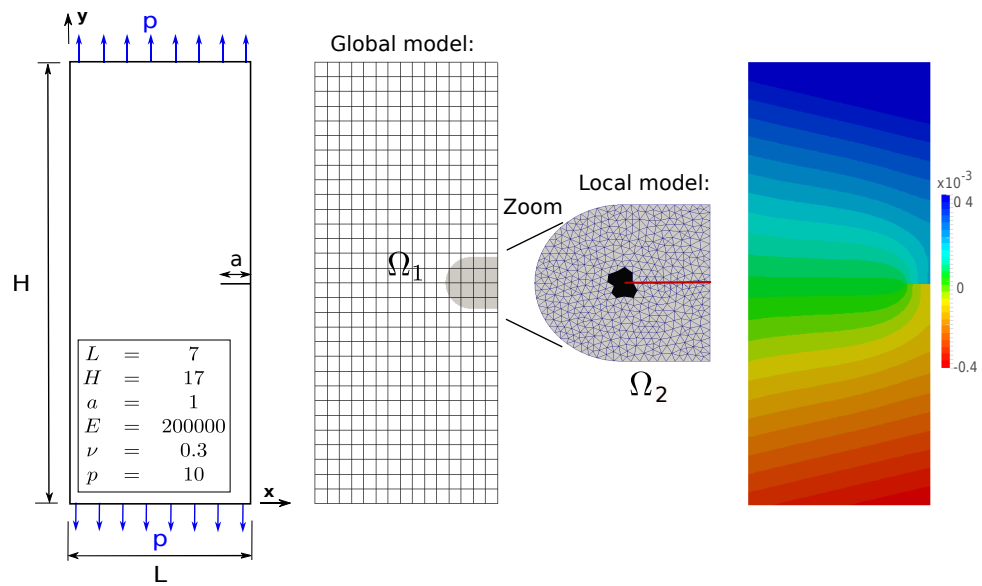
**Description of the test case:** In the last example, we demonstrate the ability of the proposed methodology to combine analysis models that consist

of several different element types coming from different numerical codes. In particular, we are interested in the coupling of NURBS elements with standard finite elements (*i.e.*, based on Lagrange shape functions). This may be of great interest for engineers because it provides a flexible tool to couple robust conventional finite element codes with newly developed NURBS codes. We recall that the procedure illustrated in Fig. 6 is used for the non-intrusive coupling. For the study, an edge-cracked plate, as shown in Fig. 18(a), subjected to a uniform tensile stress is analysed. The crack size ( $a = 1$ ) is very small in comparison with the lengths of the plate ( $H = 17$  and  $L = 7$ ), so the problem exhibits two different scales. The structure is assumed to be in plane strain conditions. Such a problem has already been studied in the context of non-intrusive FEM (see, *e.g.*, [11]). The reference value of the mode I Stress Intensity Factor (SIF) can be accurately approximated by the value that holds for an infinite plate, corrected by a factor depending on the ratio  $\frac{a}{L}$ :

$$K_I^{ref} = p\sqrt{a\pi} \left[ 1.12 - 0.231 \frac{a}{L} + 10.55 \left( \frac{a}{L} \right)^2 - 21.72 \left( \frac{a}{L} \right)^3 + 30.39 \left( \frac{a}{L} \right)^4 \right]. \quad (37)$$

**Numerical model considered:** The non-intrusive numerical model considered is illustrated in Fig. 18(b). To model the behaviour around the crack, we propose to make use of the well-established X-FEM method (in the context of usual FEM). In particular, X-FEM linear triangles are used here to discretize the local model. In addition, we propose to add an analytical domain at the crack tip in the local model, which contains the Williams' expansion [49]. The consequence of this is that the stress intensity factors can be derived directly. For details regarding crack modelling, the interested reader is invited to consult [11] and references cited therein. The local model is computed using the code of [11]. Simultaneously, a quadratic  $15 \times 30$  B-spline mesh is used in our IGA code as the global model to compute the plate without the crack. This model is intended to be replaced around the crack by the local model presented above. Non-conforming geometries are involved (see, again, Fig. 18(b)).

**Numerical results:** The vertical displacement obtained (once the non-intrusive algorithm has converged) with the discretizations of Fig. 18(b) is plotted in Fig. 18(c). A deformation similar to that in [11] can be observed. In addition, the convergence behaviour of the mode I SIF  $K_I$  with the non-



(a) Problem description. (b) Meshes: global quadratic B-Spline model (the local region in grey) and local model including X-FEM linear triangles (crack in red) and the analytical domain (black). (c) Converged solution: disp.  $u_y$ .

Figure 18: Non-intrusive analysis of an edge crack plate under uniaxial stress.

intrusive algorithm is shown in Fig. 19. We note that only five iterations are required to obtain the converged value with the Newton acceleration technique. For the discretization considered, a relative error of 0.08% on  $K_I$  with respect to  $K_I^{ref}$  (Eq. (37)) is reached. These results account for the flexibility of the method to connect finite element methods that use different basis functions. The present work can then be interpreted as an extension of the non-intrusive coupling coming from conventional FEM to higher-order finite element methods.

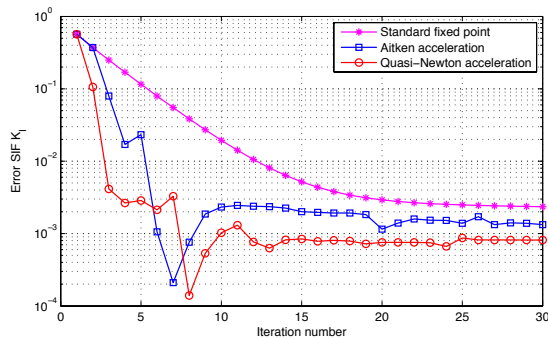


Figure 19: Convergence of the SIF  $K_I$  during the non-intrusive algorithm.

## 5. Conclusion

In this paper, we applied the global/local non-intrusive coupling strategy to the NURBS context in order to simplify the modelling of local behaviour within a NURBS patch. The idea was to consider the NURBS patch to be enriched as the global model. The first advantage of the methodology when applied to NURBS is that the global NURBS patch remains unchanged, which completely eliminates the need for costly re-parametrization procedures, even if the local domain is expected to evolve during the simulation. In addition, it should be emphasized that the global stiffness operator is assembled and factorized only once, and the system to be solved remains well-conditioned. The second advantage of the proposed approach is its considerable flexibility. Beyond being an efficient strategy to couple different element types, the formalism offers the possibility to couple different numerical codes with very little implementation effort. Since the global and local problems are solved alternately and only interface data are transmitted in a non-intrusive strategy, it is possible to use a linear NURBS code for the global model and any

other existing robust codes suitable for the modelling of complex behaviour for the local model. This notably allows for easy merging of robust conventional FEM codes with newly developed NURBS codes which, in our opinion, may foster the integration of NURBS in the engineering world.

We have presented a range of numerical examples that demonstrate the ability of the non-intrusive coupling to model various types of local behaviour within a NURBS patch. Starting with the specific case of a local model that is void, we derived a strategy for the situation of geometric details, which requires only global Neumann problems to be solved in the iterative procedure. In a second part, we investigated the more usual case of covered local models. First, we considered a refined NURBS local model to achieve local refinement, then studied the modelling of a stiffer inclusion by involving a local model with a different Young modulus and, finally, combined our linear NURBS code with a standard FEM code to incorporate a local model including standard X-FEM linear triangles for crack modelling. The results confirm that the proposed approach does not compromise accuracy. In particular, the optimal rates of convergence were achieved. The price to pay for the non-intrusive strategy is the number of iterations of the solver but we have shown that this can be reduced to a few dozen with the use of acceleration techniques (Aitken dynamic relaxation and Quasi-Newton update). In consequence, we believe that our methodology is of significant interest for treating any case of local enrichment expected to evolve in a NURBS patch.

From the non-intrusive coupling point of view, the main development from FEM to NURBS consisted of taking non-conforming geometries into account. Because of the rigid tensor product structure of NURBS, the case of a local model domain overlapping the knot-span elements in the global NURBS patch had to be investigated. To this end, we decided to stay close to the initial FEM non-intrusive strategy. We kept the same equations and associated weak forms. Thus, only slight changes in the implementation process were required. In particular, we had to set up suitable quadrature rules for the evaluation of the interface reaction forces. For the case of a void local model, we proposed the simple construction of an exact NURBS domain to fill in the geometric detail by adding multiple interpolatory control points at the center. The procedure applies directly to all types of star domains and may require a few additional improvements (such as based on very recent works [44, 45]) in the general case. For the situation of covered local models, the quadrature rule coming from the local problem was transposed within the global NURBS patch. Since NURBS usually implies higher or-

der shape functions, our developments can also be viewed as an extension of non-intrusive FEM coupling to higher-order finite element methods.

The numerical experiments of the present contribution were limited to two-dimensional linear elasticity. However, the proposed strategy does not seem to require such a framework. In particular, the case of three dimensions and nonlinear local models is straightforward as demonstrated in the context of standard FEM (see, *e.g.*, [30]) which opens the door to the tackling of realistic engineering applications. Moreover, the ability of the proposed methodology to take any modification of local models into account may constitute an attractive feature for the resolution of optimization problems. With NURBS, the non-intrusive strategy could offer a robust, flexible tool for employing a design-through-analysis method for shape optimization.

### Acknowledgements

The authors gratefully acknowledge support from the French National Research Agency under Grant ANR-12-MONU-0002 ICARE. The authors would also like to thank Pr. Patrick Laborde for fruitful discussions.

- [1] T.J.R. Hughes, J.A. Cottrell, Y. Bazilevs, Isogeometric analysis: CAD, finite elements, NURBS, exact geometry, and mesh refinement, *Computer Methods in Applied Mechanics and Engineering* 194 (2005) 4135-4195.
- [2] J.A. Cottrell, T.J.R. Hughes, Y. Bazilevs. Isogeometric analysis: Toward Integration of CAD and FEA, *Wiley* 2009.
- [3] J. Evans, Y. Bazilevs, I. Babuska, T.J.R. Hughes, n-widths, sup-infs, and optimality ratios for the k-version of the isogeometric finite element method, *Computer Methods in Applied Mechanics and Engineering* 198 (2009) 1726-1741.
- [4] J.A. Cottrell, A. Reali, Y. Bazilevs, T.J.R. Hughes, Isogeometric analysis of structural vibrations, *Computer Methods in Applied Mechanics and Engineering* 195 (2006) 5257-5296.
- [5] D. Schillinger, J.A. Evans, A. Reali, M.A. Scott, T.J.R. Hughes, Isogeometric Collocation: Cost Comparison with Galerkin Methods and Extension to Adaptive Hierarchical NURBS Discretizations, *Computer Methods in Applied Mechanics and Engineering* 267 (2013) 170-232.

- [6] D. Schillinger, M. Ruess, N. Zander, Y. Bazilevs, A. Düster, E. Rank, Small and large deformation analysis with the  $p$ - and B-spline versions of the Finite Cell Method, *Computational Mechanics* 50 (2012) 445-478.
- [7] R. Echter, M. Bischoff, Numerical efficiency, locking and unlocking of NURBS finite elements, *Computer Methods in Applied Mechanics and Engineering* 199 (2010), 374-382.
- [8] R. Bouclier, T. Elguedj, A. Combescure, An isogeometric locking-free NURBS-based solid-shell element for geometrically nonlinear analysis, *International Journal for Numerical Methods in Engineering* 101 (2015) 774-808.
- [9] V.P. Nguyen, P. Kerfriden, M. Brino, S.P.A. Bordas, E. Bonisoli, Nitsche's method for two and three dimensional NURBS patch coupling, *Computational Mechanics* 53 (2014) 1163-1182.
- [10] C.A. Duarte, D.J. Kim, Analysis and applications of a generalized finite element method with global-local enrichment functions, *Computer Methods in Applied Mechanics and Engineering* 197 (2008) 487-504.
- [11] J.C. Passieux, J. Réthoré, A. Gravouil, M.C. Baietto, Local/global non-intrusive crack propagation simulation using multigrid XFEM solver, *Computational Mechanics* 52 (2013) 1381-1393.
- [12] L. Gendre, O. Allix, P. Gosselet, F. Comte, Non-intrusive and exact global/local techniques for structural problems with local plasticity, *Computational Mechanics* 44 (2009) 233-245.
- [13] A.V. Vuong, C. Giannelli, B. Juttler, B. Simeon, A hierarchical approach to adaptive local refinement in isogeometric analysis, *Computer Methods in Applied Mechanics and Engineering* 200 (2011) 3554-3567.
- [14] D. Schillinger, L. Dede, M.A. Scott, J.A. Evans, M.J. Borden, E. Rank, T.J.R. Hughes, An isogeometric design-through-analysis methodology based on adaptive hierarchical refinement of NURBS, immersed boundary methods, and T-spline CAD surfaces, *Computer Methods in Applied Mechanics and Engineering* 249-252 (2012) 116-150.

- [15] T. Dokken, T. Lyche, K.F. Pettersen, Polynomial splines over locally refined box-partitions, *Computer Aided Geometric Design* 30 (2013) 331-356.
- [16] Y. Bazilevs, V.M. Calo, J.A. Cottrell, J.A. Evans, T.J.R Hughes, S. Lipton, Isogeometric analysis using T-splines. *Computer Methods in Applied Mechanics and Engineering* 199 (2010) 229-263.
- [17] M.A. Scott, X. Li, T.W. Sederberg, T.J.R. Hughes, Local refinement of analysis-suitable T-splines, *Computer Methods in Applied Mechanics and Engineering* 213-216 (2012) 206-22.
- [18] A. Chemin, T. Elguedj, A. Gravouil, Isogeometric local  $h$ -refinement strategy based on multigrids, *Finite Elements in Analysis and Design* 100 (2015) 77-90.
- [19] M. Ruess, D. Schillinger, A.I. Özcan, E. Rank, Weak coupling for isogeometric analysis of non-matching and trimmed multi-patch geometries, *Computer Methods in Applied Mechanics and Engineering* 269 (2014) 46-71.
- [20] D. Schillinger, M. Ruess, The Finite Cell Method: A review in the context of higher-order structural analysis of CAD and image-based geometric models, *Archives of Computational Methods in Engineering* (2015) 1-65.
- [21] C. Hesch, P. Betsch, Isogeometric analysis and domain decomposition methods, *Computer Methods in Applied Mechanics and Engineering* 213-216 (2012) 104-112.
- [22] A. Apostolatos, R. Schmidt, R. Wuchner, K.U. Bletzinger, A Nitsche-type formulation and comparison of the most common domain decomposition methods in isogeometric analysis, *International Journal for Numerical Methods in Engineering* 97 (2014) 473-504.
- [23] V.P. Nguyen, P. Kerfriden, S. Claus, S.P.A. Bordas, Nitsche's method method for mixed dimensional analysis: conforming and non-conforming continuum-beam and continuum-plate coupling, arXiv:1308.2910v1.

- [24] Y. Guo, M. Ruess, Nitsche’s method for a coupling of isogeometric thin shells and blended shell structures, *Computer Methods in Applied Mechanics and Engineering* 284 (2015) 881-905.
- [25] M. Ruess, D. Schillinger, Y. Bazilevs, V. Varduhn and E. Rank, Weakly enforced essential boundary conditions for NURBS-embedded and trimmed NURBS geometries on the basis of the finite cell method, *International Journal for Numerical Methods in Engineering* 95 (2013) 811-846.
- [26] W. Dornisch, G. Vitucci, S. Klinkel, The weak substitution method – An application of the mortar method for patch coupling in NURBS-based isogeometric analysis, *International Journal for Numerical Methods in Engineering* 103 (2015) 205–234.
- [27] J.D. Whitcomb, Iterative global/local finite element analysis, *Computers & Structures*, 40 (1991) 1027-1031.
- [28] M. Chevreuril, A. Nouy, E. Safatly, A multiscale method with patch for the solution of stochastic partial differential equations with localized uncertainties, *Computer Methods in Applied Mechanics and Engineering* 255 (2013) 255-274.
- [29] G. Guguin, O. Allix, P. Gosselet, S. Guinard, Nonintrusive coupling of 3D and 2D laminated composite models based on finite element 3D recovery, *International Journal for Numerical Methods in Engineering* 98 (2014) 324-343.
- [30] M. Duval, J.C. Passieux, M. Salaün, S. Guinard, Non-intrusive coupling: recent advances and scalable nonlinear domain decomposition, *Archives of Computational Methods in Engineering* (2014) 1-22.
- [31] J. L. Steger, F. C. Dougherty, J. A. Benek, A chimera grid scheme, *Advances in grid generation - ASME FED* 5 (1983).
- [32] R. Glowinski, J. He, A. Lozinski, J. Rappaz, J. Wagner, Finite element approximation of multi-scale elliptic problems using patches of elements, *Numerische Mathematik*, 101 (2005) 663-687.

- [33] J. B. Apoung Kamga, O. Pironneau, Numerical zoom for multiscale problems with an application to nuclear waste disposal, *Journal of Computational Physics*, 224 (2007) 403-413.
- [34] E. Rank, Adaptive remeshing and h-p domain decomposition, *Computer Methods in Applied Mechanics and Engineering* 101 (1992) 299-313.
- [35] E. Rank, A zooming-technique using a hierarchical hp-version of the finite element method, J. Whiteman (Ed.), *The Mathematics of Finite Elements and Applications-Highlights 1993*, Elsevier, Uxbridge 1993.
- [36] A. Düster, A. Niggel, E. Rank, Applying the hp-d version of the FEM to locally enhance dimensionally reduced models, *Computer Methods in Applied Mechanics and Engineering* 196 (2007) 3524-3533.
- [37] E. Cohen, T. Lyche, R. Riesenfeld, Discrete B-spline and subdivision techniques in computer aided geometric design and computer graphics, *Computer Graphics and Image Processing*, 14 (1980) 87-111.
- [38] L. Piegl, W. Tiller, *The NURBS Book* (Monographs in Visual Communication), second ed., Springer-Verlag, New York, 1997.
- [39] G. Farin, *Curves and Surfaces for CAGD, A Practical Guide*, Fifth Edition. Morgan Kaufmann Publishers 1999.
- [40] D.F. Rogers, *An introduction to NURBS With Historical Perspective*, Academic Press, 2001.
- [41] J.A. Cottrell, T.J.R. Hughes, A. Reali, Studies of refinement and continuity in isogeometric structural analysis, *Computer Methods in Applied Mechanics and Engineering* 196 (2007) 4160-4183.
- [42] N. Moës, J. Dolbow, T. Belytschko, A finite element method for crack growth without remeshing, *International Journal for Numerical Methods in Engineering* 46 (1999) 131-150.
- [43] R. Sevilla, S. Fernández-Méndez, A. Huerta, NURBS enhanced finite element method (NEFEM), *International Journal for Numerical Methods in Engineering* 76 (2008) 56-83.

- [44] A.P. Nagy, D. J. Benson, On the numerical integration of trimmed isogeometric elements, *Computer Methods in Applied Mechanics and Engineering* 284 (2015) 165-185.
- [45] L. Kudela, N. Zander, T. Bog, S. Kollmannsberger, E. Rank, Efficient and accurate numerical quadrature for immersed boundary methods, *Advanced Modeling and Simulation in Engineering Sciences* (2015) 2:10.
- [46] M.H. Sadd, Elasticity, Theory, Applications, and Numerics, *Academic Press, Oxford* 2009.
- [47] Electricite de France, Code-Aster (2014) URL <http://www.code-aster.org>.
- [48] O.C. Zienckewicz, R.L. Taylor, The Finite Element Method - The Basis, vol.1, *Butterworth-Heinemann*, 2005, sixth ed..
- [49] J. Réthoré, S. Roux, F. Hild, Hybrid analytical and extended finite element method (HAX-FEM): A new enrichment procedure for cracked solids, *International Journal for Numerical Methods in Engineering* 81 (2010) 269-285.